CHITECTS AND MARINE ENGINEERS
/. 10006

no. 12

Advance copy of paper to be presented at the Annual Meeting, New York, N. Y., November 11–13, 1976

Influence of Major Characteristics of Icebreaker Hulls on Their Powering Requirements and Maneuverability in Ice

R. Y. Edwards, Jr.,[1] Member, **R. A. Major,**[2] Member, **J. K. Kim,**[2] Member, **J. G. German,**[3] Member, **J. W. Lewis,**[2] Associate Member, and **D. R. Miller,**[4] Life Member

The Canadian Coast Guard has undertaken the design of a large polar icebreaker. To ensure that high performance in ice would be achieved in this ship, the Canadian Coast Guard commissioned a hull development program to determine, through systematic tests in ice, the influence of designer-controlled variables such as beam, length, draft, block coefficient, and possibly hull-ice friction factor upon icebreaking performance and maneuverability, and to use the results of the experimental program to select the major dimensions and propulsive power of the icebreaker. The program was divided into four parts: A model/full-scale correlation study, parametric ice resistance tests, assessment of icebreaker maneuverability, and selection of least-cost hull parameters and power. In the course of the program, correlation was demonstrated between model prediction techniques and full-scale observations in ice thicknesses up to six feet. Parametric ice resistance experiments revealed that draft and block coefficient exert a significant effect on icebreaker performance in level ice. A modified rotating arm experimental/analysis technique was developed to assess the maneuverability of ships in level ice. Model predictions of turning circle were found to reproduce full-scale turning circle measurements well. Parametric maneuvering model tests revealed that a steady-state turning circle in level ice increases markedly with increasing ice thickness, ship length, and block coefficient. The ice resistance equation developed from the parametric test results was used in an optimization program to provide the main dimensions, power, and estimated cost of a least-initial-cost large polar icebreaker.

Introduction

Background

CANADA's decision to design a large icebreaker was taken because of the very considerable increase in probable future activities in Arctic regions, the realization of which came rather rapidly after oil was discovered at Prudhoe Bay and iron ore in Baffin Island.

A combination of national and world shortages and Arctic discoveries made it fairly certain that, in a short space of time, the development of Arctic regions is inevitable. In a new consciousness of the importance of these regions and the probability of near-term development imperatives, a disquieting awareness grew of the fact that Canada does not have icebreakers capable of operating in the Arctic regions beyond the 4- to 5-month summer period.

With resource companies talking about bringing gas and oil out by the early 1980's and minerals even sooner than that, the need to plan for the building of an icebreaker support facility became extremely urgent. This facility also had to be far more ice-capable than anything existing in the Canadian icebreaking fleet and, indeed, the world.

The Canadian Government, therefore, took the decision almost two years ago to proceed with the design development of a powerful new icebreaker suited to operating at least ten months of the year in the lower Arctic regions and which could effectively act as a support tool for extended season Arctic shipping.

Need for optimization

It was realized that the vessel would have to be three to four times as capable and powerful as Canada's existing largest icebreaker, the *Louis S. St. Laurent*, which itself ranks among the world's most powerful icebreakers. The prospect for the new vessel, which became termed *Polar VII*, was that it would be an expensive ship but, nevertheless, essential to the development of Canada's Arctic. The capital cost was initially estimated between $150 and $200 million. The ship would therefore cost almost an order of magnitude more than any existing ship in the Canadian icebreaking fleet! The estimated 20-year life-cycle costs were equally impressive. However, the requirement for a ship of this capability to fill the role of supporting the expected development of Arctic shipping left no alternative.

Because of the anticipated magnitude of the investment in the *Polar VII*, it was apparent that optimization of the design could yield a significant economic benefit. If by improving the intrinsic icebreaking capability of the ship by, say, an improved hull shape, it were possible to reduce the required displacement of the ship by ten percent and still have a ship which met operational requirements, a savings of $10 to $15 million in capital cost would result, to say nothing of the reduction in life-cycle costs. On the other hand, an arbitrary reduction in

[1] ARCTEC Canada Limited, Montreal, Quebec.
[2] ARCTEC, Incorporated, Columbia, Maryland.
[3] German and Milne, Montreal, Quebec.
[4] Transport Canada, Canadian Coast Guard, Ottawa, Ontario.

For presentation at the Annual Meeting, New York, N. Y., November 11–13, 1976, of THE SOCIETY OF NAVAL ARCHITECTS AND MARINE ENGINEERS.

BY THE SOCIETY OF NAVAL ARCHITECTS AND MARINE ENGINEERS

Table I Influence of variations in independent variables on acquisition costs as estimated by a feasibility icebreaker design mathematical model

Variable	Effect on cost if variable is increased	Sensitivity[a]
L/H	increased	0.013
B/H	increased	0.252
Δ	increased	0.745
C_B	decreased	−0.879
C_p	no change	. . .
SHP/Δ	increased	0.266

[a] Increment in cost/base cost / Increment in variable/base value of variable

size or power of the *Polar VII* might reduce the icebreaker's capability to support shipping, increasing the costs to all shipowners who would depend on it.

Icebreaking performance

In order to optimize the design of a ship intended for ice operations it is necessary to have available data that express the performance of the ship not only in terms of the important parameters describing the ice environment, but also in terms of those properties of the ship which strongly influence cost and which are suspected to influence performance.

Melberg et al [1][5] presented the results of a computer program for selecting a least-cost icebreaker. A summary of their findings is given in Table 1. These results suggest that the block coefficient and breadth-to-draft ratio are major hull form parameters which influence costs significantly.

At the time the design of the *Polar VII* was awarded, there were three main sources of information on predicting the performance of ships in ice: the work of the Soviets, which is well summarized by Kashtelyan et al [2]; the U.S. studies reported by Lewis and Edwards [3–5] and Kotras and Benze [6]; and the combined works of Enkvist [7] and Johanssen and Makinen [8].

All of these sources contributed significantly to the state of the art of estimating the powering requirements for icebreaking ships. However, without prejudicing the efforts of these investigators, the empirical and analytical predictors which were available to the authors were not adequate for the task of optimizing the hull design of the *Polar VII*. Specifically:

- Only Johanssen's and Makinen's work incorporated tests to assess by model test the effect of ship breadth on resistance to motion in level ice. Furthermore, their work was carried out on ore carrier forms with high values of C_B and L/B. It was suspected that their findings would not accurately apply to the *Polar VII* hull because of the great difference in hull form compared with ore carrier hull forms.
- No systematic assessment of the effect of block coefficient on resistance in level ice had ever been carried out.
- The results of tests by Kotras and Benze [6] and Johanssen and Makinen [8] to assess the effect of ship length on level ice resistance were for wall-sided ships with very long parallel middlebody. The results of the two in combination did not produce unequivocal predictors of the L/B effect.
- No satisfactory results of tests to assess the effect of draft variation on level ice resistance were available in a usable form.
- Bow shape: Kashtelyan's semi-empirical ice resistance predictor equations [2] compared favorably with full-scale data gathered on a very narrow range of forebody shapes, while Johanssen's and Makinen's test results dealt with large stem slope changes on bulk carrier forms rather than the more subtle changes in bow shape germane to icebreaker bow shape optimization.

In summary, the designer had available semi-empirical predictors for resistance in level ice. However, these tools included a logical but uncorroborated linear dependence of resistance on beam and did not incorporate a capability to assess the effect on ice resistance of B/H, L/B, and C_B, variables which markedly effect the cost of the ship. Basically the designer's tasks required a "Taylor's Standard Series for Icebreaking," but none existed. Consequently, it was considered in the best interests of the owner to conduct extensive ice resistance experiments to assess the influence of variation in hull parameters, which were suspected to have a significant effect on construction costs, and upon icebreaking performance. Further, the results of this experimental program were to be used in conjunction with an initial cost optimization program to check the initial selection of the major hull form parameters of the *Polar VII*.

Maneuverability constraints

The maneuverability of an icebreaker used for shipping escort is very important. At the time of the initiation of the design study, no rational techniques existed for assessing the influence of hull parameters on maneuverability in ice. Of course, icebreaker designers realized by intuition that length between perpendiculars and the length of parallel middlebody influence the turning capability of an icebreaker, but there were no data or mathematical model which could be used to determine, quantitatively, the effect which changing length or block coefficient would have on maneuverability. Consequently, the development of a technique to predict maneuverability in level ice—and to use the technique to assess the effect of changes in ship length and block coefficient on turning circle and directional stability—was incorporated in the experimental program. Although the results of this work could not be used directly in the optimization program, they would serve as an external constraint or check to ensure that a hull form selected to maximize icebreaking performance (level ice resistance on a constant heading) and to minimize cost would not exhibit unacceptable maneuvering characteristics.

Model/full-scale correlation and media selection

At the time of the initiation of the study, a facility suitable for ship towing tests was available in Canada which was set up to use a synthetic ice recently developed by Michel [9]. The material was attractive mainly because the ratio of elastic modulus to bending strength was quite close to that of real ice, whereas it was difficult in saline ice to achieve levels of this parameter equal to those attributed to full-scale ice. However, the material was relatively untried as a media for ship model testing. Modeling the interaction between sloping structures and ice had, however, been successfully undertaken.

The prospect of conducting the experimental program in a local facility was attractive as was the potential of the synthetic ice. Consequently, a part of the program was devoted to assessing the suitability of synthetic ice for icebreaker performance modeling.

Ship model tests which consist in measuring the performance of ship models in ice covers frozen on salt water had been shown by Edwards et al [4] to exhibit reasonable model/full-scale correlation, at least for *Wind*-Class icebreakers and in ice the full-scale thickness of which did not exceed two feet. The *Polar VII* was intended to operate in seven feet of ice!

The only full-scale data available to the designer for ice thicknesses approaching that level were obtained during trials of the CCGS *Louis S. St. Laurent* in 1970. Consequently, a series of model/full-scale correlation tests involving the *St. Laurent* was incorporated in the experimental program to

[5] Numbers in brackets designate References at end of paper.

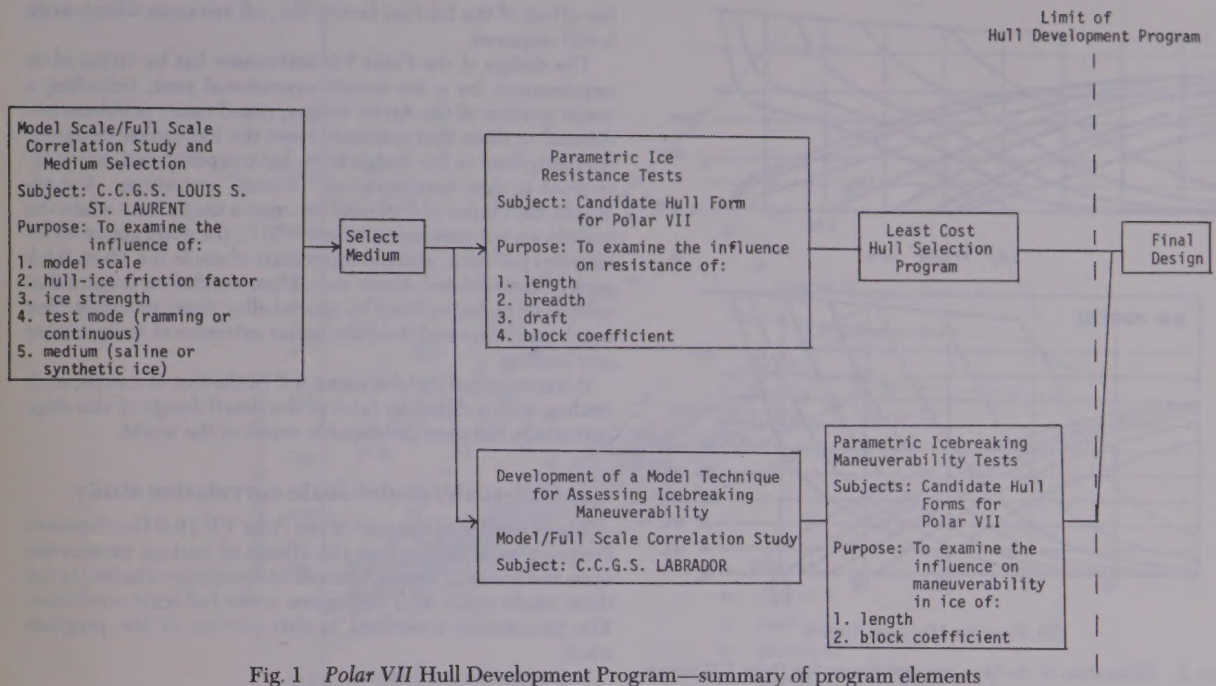

Fig. 1 *Polar VII* Hull Development Program—summary of program elements

support the design of the *Polar VII*.

The effect of scale on the correlation of model ice resistance with full-scale ice resistance had been investigated by Kashtelyan et al [2]. His results showed a dispersion between resistance predictions from 1:65, 1:80, and 1:50 scale models which increased from almost zero at very low Froude number to 20 percent or more at high Froude number but which did not exhibit a consistant relationship with geometric scale factor. An investigation into the effect of geometric scale factor on the accuracy of ice resistance prediction was included in the program.

To summarize, before undertaking the experiments to assess the effect of variations in selected hull parameters on resistance to motion and maneuverability in level ice, a program of tests was undertaken to evaluate the following:

- Relative suitability of model tests in synthetic and saline ice for predicting full-scale performance.
- Effect of geometric scale ratio on predicted full-scale resistance.

These preliminary tests, parametric resistance and maneuvering tests, and exercise of the program for selecting least-cost icebreaker parameters for a given mission were combined into a program referred to as the Hull Development Program.

Hull Development Program

Figure 1 illustrates the logic sequence for the Hull Development Program. It consisted of the (*a*) preliminary correlation and media selection program, (*b*) parametric resistance tests, (*c*) development of a model technique for assessing icebreaking maneuverability, (*d*) parametric icebreaking tests, and (*e*) least-cost hull selection program.

It was realized that time and budget would not permit a development program which could yield a complete set of data for the effect of changing hull form parameters. *Polar VII* was to be designed within a time constraint which would be tight even were the methods for estimating power requirements as advanced as for open-water calculations.

It was decided at the outset of the program, therefore, to limit the testing program to provide data sufficient to produce predictor formulas which allowed for the influence of the following variables on icebreaking resistance:

1. Length
2. Breadth
3. Draft
4. Block coefficient

These variables were the primary ones to be investigated for a hull form series which had the following fixed parameters, variations of which were not to be investigated:

1. Fixed midship section flare angle
2. Fixed rise of floor angle
3. Stem profile
4. Stern design
5. Location of longitudinal center of bouyancy

The concept selected by the Canadian Coast Guard for the stem design was the so-called "White bow," shown in previous tests [5, 9] to be superior to a normal icebreaker bow form having straight stem profile with a rake angle of approximately 26 to 30 deg. In Fig. 2, the difference between the selected bow concept [Fig. 2(*a*)] and the traditional icebreaking bow shape [Fig. 2(*b*)] is illustrated.

The target of the program was to develop an icebreaker design which would meet the following performance requirements:

Icebreaking performance:

Continuous mode—3 knots in 7-ft-thick consolidated pack ice.

Ramming mode—in consolidated pack ice up to 25 ft thick.

Open-water performance:

Cruising radius—Minimum of 20,000 nautical miles at economical speed in open water with 20 percent fuel remaining.

Constraints:

Restraint on draft—not to exceed 45 ft.

Restraint on breadth—not to exceed 106 ft overall (Panama Canal Authority).

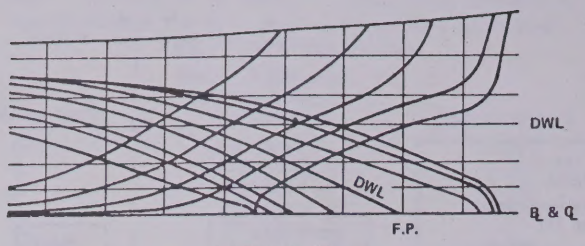

(*a*) "White" bow

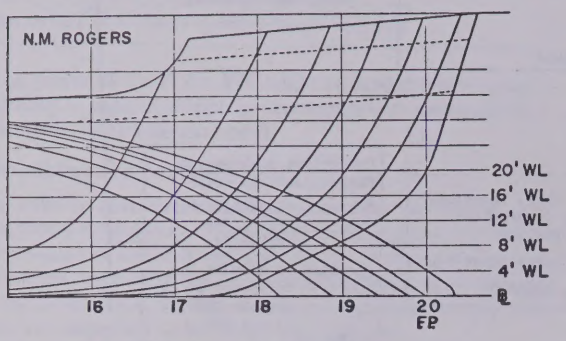

(*b*) *Norman McLeod Rogers*

Fig. 2 Illustration of the bow concept chosen for *Polar VII* versus traditional *Wind*-Class type bow

Costs:
Minimum capital cost.
Minimum 20-year life-cycle costs.

The hull development program and its results are documented in the following pages. It seems a curious fact that such programs have not been undertaken before now, and the authors wish to express their respect for the officials of the Canadian Coast Guard who saw the need and sponsored the program.

Conclusion

The results available to the Canadian Coast Guard from this, the first published series of systematic tests on a family of icebreaker forms, have already proved most useful and have justified the application of a major portion of their research funds into this type of program. Up to this time, data available have tended to be applicable to one specific ship rather than to a family or series. Now for the first time the designer has been given a tool to allow him, during the design spiral, to measure with confidence the effect on icebreaking performance and thus cost effectiveness of any envelope modification contemplated to the vessel. During the development of the *Polar VII* design, all changes in dimensions, form, or power were assessed for effect on the overall performance in ice, both in level ice resistance and in maneuvering criteria. The result will be a more efficient vessel to the owner, representing the best compromise between his conflicting requirements of maximum performance in Arctic ice, the capability of entering shallow rivers and fjords and fitting into existing servicing equipment and methods, while at the same time having a minimum capital and annual operating cost.

Although much has been achieved under this program, the authors realize that many factors still remain to be investigated before a documented series of icebreaker forms is available to naval architects, comparable to the standard series already in use throughout the world for open-water performance. The influence of bow shape, flare angle both forward and amidships, the effect of the friction factor, etc., all are areas where work is still required.

The design of the *Polar VII* icebreaker has by virtue of its requirement for a ten-month operational year, including a major portion of the Arctic winter, posed many problems additional to those that normally beset the icebreaker designer. All disciplines in the design team have experienced major extensions to their boundaries of "normal" operations. For example, the choice of hull steel becomes a major item when the outside air temperature is below −50 C, the wind above 90 kilometers per hour, and the immediate obstacle is a 10-m-thick pack of consolidated Arctic ice! These conditions require that normal steels be replaced by special alloy steels retaining their notch toughness and ductility under extremes of temperature and loading.

It is anticipated that this paper will be the first of a series, each dealing with a different facet of the detail design of this ship, potentially the most ice-capable vessel in the world.

Full-scale/model-scale correlation study

The objectives of this part of the *Polar VII* Hull Development Program were to examine the effects of various parameters upon the results of model tests and to determine whether or not these results agree with data taken under full-scale conditions. The parameters examined in this portion of the program were:

- Geometric scale factor.
- Ice strength.
- Hull-ice friction factor.
- Test mode, that is, constant-velocity towed or ramming/penetration mode.
- Test media, that is, saline ice or synthetic wax-based model ice.

Geometric scale factors of 36 and 48 were used during this part of the program. Smaller geometric scale factors give larger, easier to measure test forces and use closer to full-scale property values which allow more accurate scaling of the ice properties, particularly the elastic modulus. With larger geometric scale factors, a greater number of test data points may be obtained from a given length of model ice. It is also possible above certain scale factors to test two models side by side in the model basin, and thus double the number of data points per test ice sheet. The effects of variation in the flexural strength of the ice cover were examined over the ranges observed in Arctic ice. The importance of hull-ice friction has recently gained a great deal of attention and it is expected that the condition of the snow cover itself during full-scale trials may play an important part in the results of full-scale tests. The model series was therefore designed to cover a range of hull-ice friction which would encompass all possible full-scale conditions from that of a low friction coating to a very sticky snow cover against the pitted bare hull steel. Several investigators have advocated the use of ramming or deceleration tests in lieu of constant-velocity tests for full-scale testing of new hull forms, and so the test program was designed to test the same hull form in both the constant-velocity mode and in a ramming or deceleration mode. In this way comparisons of results obtained from each type of testing can give predictors for continuous motion. At the time of this program, no extensive ship model tests had been conducted in a new synthetic modeling material which more closely simulated true ice elastic modulus. The test program was therefore made to include tests in this new synthetic ice material in order to determine if, in fact, better results could be obtained with it than with saline ice material.

The ability to test models of ice-transiting ships in model basins and project the results to full-scale performance has been

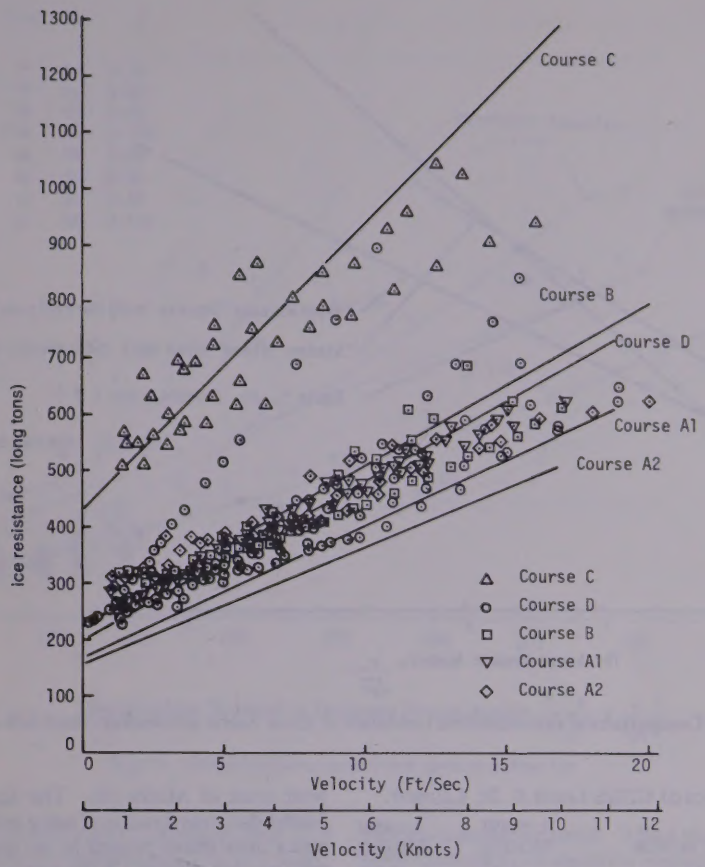

Fig. 3 Full-scale resistance data for CCGS *Louis S. St. Laurent* in snow-covered ice with regression lines from combined data

developing very rapidly over the past ten years. Initial tests for icebreaking hull forms were performed in freshwater ice, paraffin wax, and saline ice. The pioneering work of Kashtelyan et al [2] in testing ice-transiting hull forms in saline ice is still used as the basis of most of today's work. Other attempts were made to test ice-transiting hull forms in paraffin wax [11], and freshwater ice [5]. The first attempt to project the results from saline ice on a dimensionless basis to full-scale results was made by Lewis and Edwards in a presentation before the Society in 1970 [3]. Also, Enkvist did some early investigation of the effect of scale [7]. Edwards, et al collected a large volume of full-scale data on an icebreaker operating in freshwater ice and compared these data with tests done in model basins with saline ice [4]. Recently, Vance [12] assembled all available full-scale data that can be correlated with model data, from which he derived and published a common equation for predicting full-scale behavior from model tests. The shortcoming of these early attempts at correlating full-scale and model-scale test results is the very severe shortage of data. In view of that, this program was designed to collect a sufficient amount of data such that the scatter which is normally seen in ice model tests would not be so great as to hide the trend of change with each of the parameters of the investigation.

A hull form was needed for this model/full-scale correlation study on which an extensive amount of full-scale data had been collected that would be relevent to the proposed operation of the new polar icebreaker under consideration. Data were available on only three arctic icebreakers: the Canadian Coast Guard ship *Louis S. St. Laurent*, the Soviet ships *Valdisvostok* and *Moskva*, which are of the same hull form, and data collected off the west coast of Alaska on the U. S. Coast Guard icebreaker *Staten Island*. Only the data on the *Louis S. St. Laurent* had been collected in the Canadian Arctic, where the new icebreaking hull form was to operate. The *St. Laurent* data had been collected under ice conditions which were greater than the limiting continuous capability of the power plant on board. Thus the data had been collected on ramming penetrations under full power. Prediction of the continuous-mode resistance from these ramming tests was made using the deceleration force in addition to the thrust of the propellers to compute the resistance of the ship at the instantaneous velocity. A set of data points was obtained by using each two-second period of those penetrations on which the ship progressed at least half of its length into an unbroken ice cover. The resistance, velocity, and ice strength at each one of these data points were formed into a dimensionless group using the Edwards, et al, method of nondimensionalizing data so they could be compared directly with data from other ship hulls having different dimensions and also with model data. The dimensionless groups thus formed were then subjected to regression analysis. The resulting equation is

$$\frac{R}{\rho_w g B h^2} = 4.242 + 0.05033 \frac{\sigma_f}{\rho_w g h} + 8.948 \frac{v}{\sqrt{gh}} \qquad (1)$$

This equation is plotted in Fig. 3, using the actual values for ice thickness and ice strength obtained during each of the five test courses where full-scale data were obtained. The data used to create the equation are also shown. The worst match with

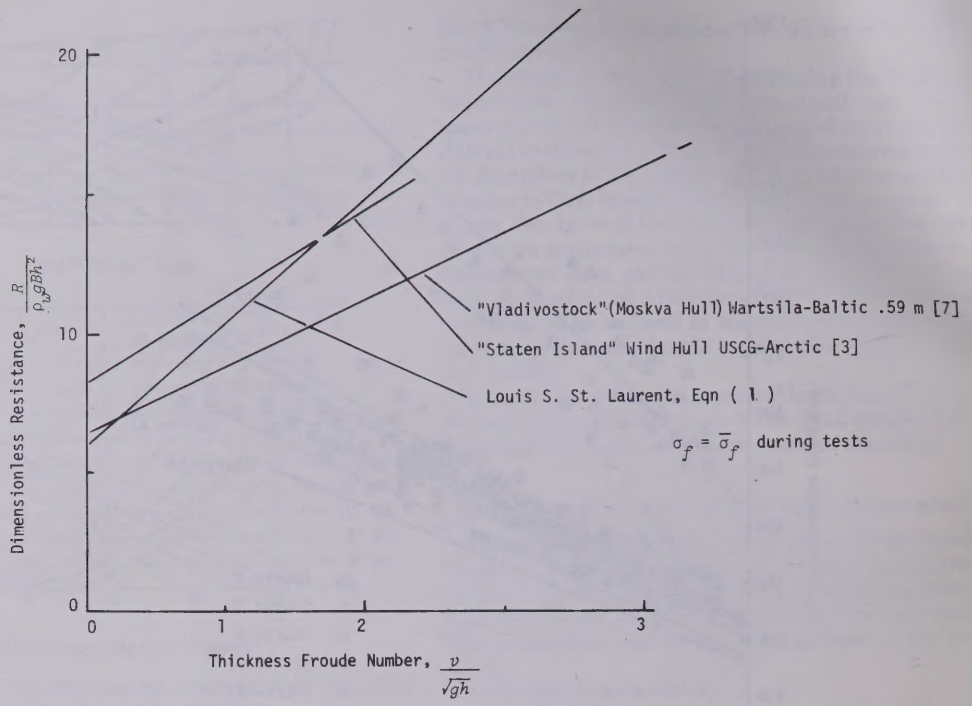

Fig. 4 Comparison of dimensionless resistance of three Arctic icebreakers from full-scale data

Table 2 Characteristics of CCGS *Louis S. St. Laurent*

	Full Scale	1/36th Model	1/48th Model
Length *BP*, ft	334.0	9.28	6.96
Beam, ft	80.0	2.22	1.67
Draft, ft	29.5	0.82	0.61
Displacement	13,300 (tons)	638.55 (lbs)	269.39 (lbs)
Block coefficient	0.59	0.59	0.59
Bow (rake) angle at test waterline, deg	32	32	32
Shimanski-Kashtelyan hull coefficient, μ_0	1.995	1.995	1.995
Shimanski-Kashtelyan hull coefficient, η_2	2.29	2.29	2.29

the data seems to have occurred in Courses A1 and A2. (The lines on Fig. 3 are for the combined data regressed nondimensionally.) A possible explanation for the higher resistance than expected which was observed on these courses might be that the ice was under some pressure during this particular run or that sun had melted the snow, resulting in higher hull-ice friction. The predictor equation seems to represent the effect of velocity quite well both in the thickest ice represented by Course C and in the medium thickness of ice represented by Courses B and D. In Fig. 4, the performance of the *Louis S. St. Laurent* is compared with two other icebreakers on which full-scale test data have been published for operations in the Arctic. In order to eliminate the effects of hull size, this figure is plotted with the resistance nondimensionalized and the velocity nondimensionalized as a thickness Froude number. The regression equation for the *St. Laurent* is plotted, and along with this are plotted the test data collected by Wartsila Helsinki Shipyard shortly after delivery of the icebreaker *Vladisvostok* [7] and tests made on the U. S. Coast Guard *Wind*-Class icebreaker *Staten Island* during February/April of 1969 off the west coast of Alaska [3]. The line representing the *Staten Island* data was developed using only those data on which there was a snow cover present at the time of the test. Snow cover was present during all the tests with the *St. Laurent*. The performance of the *St. Laurent* over the range of most of the data collected falls between that of the *Vladisvostok* and the *Staten Island*. The relatively higher velocity dependence of the hull form of the *Louis S. St. Laurent* may be due to its high block cofficient, imposed by operational requirements, and thus less advantageous breaking form of the bow. The lower resistance seen by the *Moskva* hull form on the *Vladisvostok* may be due to either a lack of snow cover on the ice in which the hull was tested or to the relatively new condition of the bottom, having just emerged from the builder's yard.

Saline ice tests

In this part of the Hull Development Program for the new Canadian polar icebreaker, the objective was to use the relatively well-established method of testing ship models in saline ice to determine the effect of scale, the effect of type of testing, the effect of ice strength, and the effect of hull-ice friction on predicted resistance in level ice. Table 2 gives the dimensions of the two models used for these tests in comparison with the full-scale dimensions of the *Louis S. St. Laurent*. The purpose of the comparison was to examine whether there was a sufficiently better comparison with tlhe full-scale data using the smaller-scale (larger) model to justify the reduced number of data points which can be obtained using it rather than the larger-scale (smaller) model. All of the full-scale data were collected using the method of ramming into an ice sheet the thickness of which was greater than the maximum continuous thickness capability of the propulsion plant. Therefore, it was deemed necessary to test the *Louis S. St. Laurent* in ramming-type tests in model scale similar to those from which the full-scale data were collected, as well as in routine constant-velocity towing tests. The full-scale range of the test data in

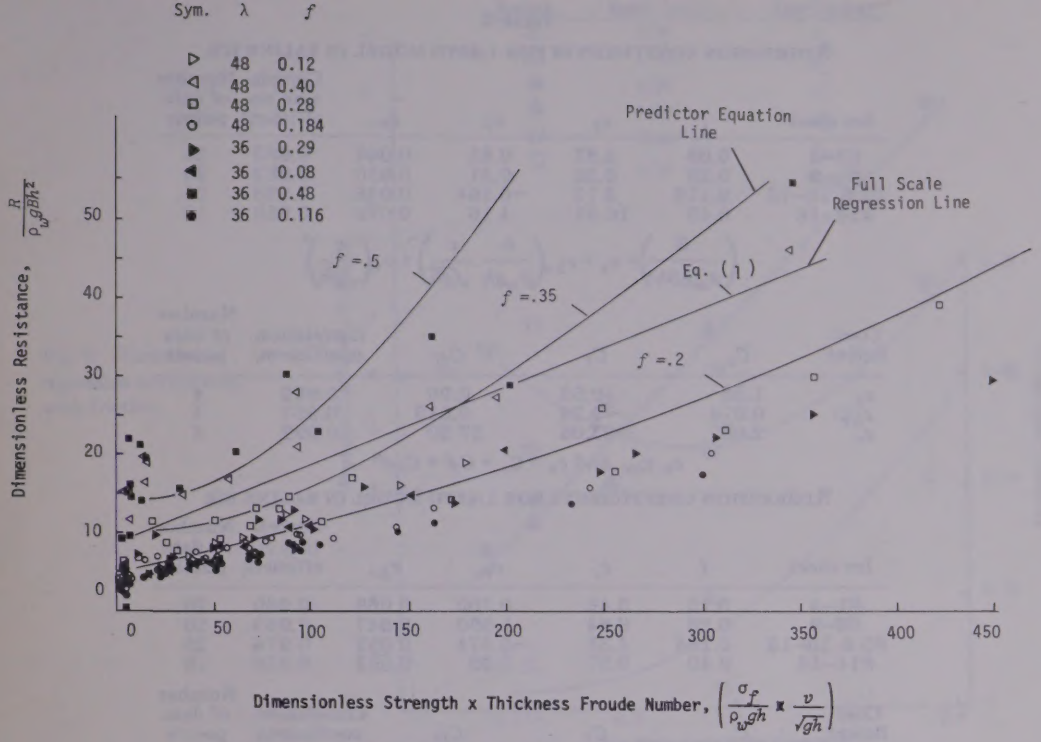

Fig. 5 Dimensionless model test data in saline ice

thickness was from 1 to 6.3 ft full scale, in strength from 45.5 to 239 pounds per square inch, in speed from 0.2 to 10.7 knots, and in hull-ice friction from 0.8 to 0.48.

The first series conducted was constant-velocity towing tests. Data from these tests are contained in the Appendix. The procedure used is identical to that described in earlier papers [4]. There are two separate sets of data corresponding to each of the two scale models. These data from both of the scale models have been plotted on a dimensionless basis in Fig. 5. The data have been grouped according to eight separate friction groups, four for each model. Black data points represent the $\frac{1}{36}$th scale model while open data points are for the $\frac{1}{48}$th model. On the ordinate the resistance is plotted while along the abscissa is plotted the product of dimensionless strength and the thickness Froude number, which, during regression analysis, was found to be the only term that contributed to resistance with a statistical level of greater than 95 percent. The predictor equation is plotted on Fig. 5 for three separate values of friction factor. Also plotted against the data and the predictor equation is the full-scale regression equation obtained from the full-scale test data.

The data collected during these tests were combined into dimensionless groups of elastic modulus over strength, E/σ_f; the thickness Froude number or velocity divided by the square root of the product of gravity and thickness, $v\sqrt{gh}$; the flexural strength divided by weight density times thickness, $\sigma_f/\rho_w gh$; and the dimensionless resistance, or resistance divided by weight density times beam and thickness squared, $R/\rho_w gBh^2$. The data were first separated into groups of like hull-ice friction. Each of these groups was subjected to stepwise multiple regression analysis to determine what terms might be important in predicting the full-scale resistance. It was found in this multiple regression analysis that only two terms were significant at the 90 percent level of confidence. These are the thickness Froude number times dimensionless strength and the thickness Froude number squared. All of the eight data sets collected were force-fit to an equation containing both of these groups. The results of this analysis are detailed in Table 3. It can be seen from Table 3 that the number of data points in each regression was approximately the same. A coefficient was obtained for each term in the hypothetical predictor equation, giving a total of eight separate values for each coefficient, corresponding to eight values of friction. A plot of these coefficients is shown in Fig. 6. Each of these coefficients was then fitted to a polynomial in hull-ice friction. Individually for each of the models and for both of the models combined, the results of these fits are given in Table 3. From these coefficients, predictor equations can be constructed which are good for each of the individual models and one which represents both models combined.

Following this program, a series of non-self-propelled ramming tests was held. It was found from these tests that the results obtained from reducing the inertial ramming tests produced data equivalent to those collected during constant-velocity towing tests. All of the data from these tests are presented in the Appendix; however, only the results of one test have been plotted in Fig. 7, where they have been converted to full-scale resistance versus velocity. Also plotted in Fig. 7 is a line corresponding to the predictor equation for the combined model data collected in continuous-icebreaking tests. The predictor equation includes values for hull-ice friction and ice strength measured during the ramming tests. At this one strength and one ice thickness, to have as much as 50 percent scatter in the magnitude of resistance indicates much poorer quality than has routinely been obtained through the constant-velocity method of testing. We therefore see that, although the results agree on a general basis and indicate that there are no strange phenomena happening during the ramming process, this method of collecting data does not hold as much promise in the model scale as the normally used constant-velocity towing method.

Table 3

REGRESSION COEFFICIENTS FOR 1/36TH MODEL IN SALINE ICE

Ice sheet	f	c_s	c_v	c_{bv}	Correlation coefficient	Number of data points
#1–4	0.08	2.87	0.85	0.064	0.983	20
#6–9	0.29	6.23	0.31	0.050	0.982	20
#5 & 10–13	0.116	3.72	−0.164	0.046	0.988	25
#14–16	0.48	10.91	4.16	0.076	0.958	18

$$\left(\frac{R}{\rho_w g B h^2}\right) = c_s + c_{bv}\left(\frac{\sigma}{\rho_w g h} \cdot \frac{v}{\sqrt{gh}}\right) + c_v\left(\frac{v}{\sqrt{gh}}\right)^2$$

Coefficient	C_0	C_f	C_{ff}	Correlation coefficient	Number of data points
c_s	1.22	19.53	0.00	0.982	4
c_{bv}	0.074	−0.24	0.513	0.957	4
c_v	2.08	−23.06	57.20	0.992	4

c_s, c_{bv}, and $c_v = C_0 + C_f f + C_{ff} f^2$

REGRESSION COEFFICIENTS FOR 1/48TH MODEL IN SALINE ICE

Ice sheet	f	c_s	c_v	c_{bv}	Correlation coefficient	Number of data points
#1–4	0.12	3.46	0.700	0.069	0.969	20
#6–9	0.28	6.84	1.890	0.047	0.963	20
#5 & 10–13	0.184	4.38	−0.074	0.052	0.976	25
#14–16	0.40	9.37	5.33	0.053	0.936	18

Coefficient	C_0	C_f	C_{ff}	Correlation coefficient	Number of data points
c_s	0.65	21.76	0.00	0.997	4
c_{bv}	0.110	−0.44	0.745	0.983	4
c_v	2.72	−29.39	90.30	0.990	4

REGRESSION COEFFICIENTS FOR COMBINED MODEL DATA

Coefficient	C_0	C_f	C_{ff}	Correlation coefficient	Number of data points
c_s	1.04	20.21	0.00	0.99	8
c_{bv}	0.083	−0.276	0.534	0.80	8
c_v	0.625	−6.45	33.14	0.86	8

Figure 8 has been constructed using the predictor equations developed for each individual model and comparing them versus thickness Froude number and strength at a fixed value of hull-ice friction. This graph shows that, at the Froude numbers normally associated with the limiting capability of the ship, the results given by the 36th and 48th scale models are nearly identical. As speed increases and we move toward thinner ice thicknesses, the predictor given by the smaller test model (1/48th scale) gives a more conservative resistance. The effect of strength can be seen by this figure to be practically negligible with regard to the prediction of either model.

Synthetic ice tests

At the time this program was started, a new synthetic testing material, developed by Dr. Bernard Michel at Laval University in Quebec, was available, and it appeared to have promise of giving better results than saline ice for ship model tests. No comprehensive ship model test, however, had ever been run in this material until this time. The material was expected to give better results than the saline ice tests primarily because of its better capability of modeling elastic modulus; that is, the material was stiffer than saline ice when the proper strength was reached for scaling.

Tests on the two *Louis S. St. Laurent* models were the first ones accomplished in the new ARCTEC CANADA ice basin using synthetic ice as a testing medium. The tests were conducted in exactly the same manner as was used in saline ice in Columbia, Maryland. The full-scale range of the properties varied during the tests: thickness ranged from 1.2 to 4.9 ft, speed from 0.6 to 12.6 knots, and flexural ice strength from 88.2 to 902 pounds per square inch. The data from this test series are also contained in Appendix 2. Initial analysis of these data on a nondimensional basis revealed that the ice tests were not showing what previous saline ice tests had indicated was the normal variation with ice thickness. The dimensionless groups did not seem to eliminate the scatter which is normally found in data taken at a number of different thicknesses. Therefore, the test data were extrapolated to full-scale levels and analyzed in the full-scale domain on a dimensional basis. The results of this analysis are given in Table 4. Hull-ice friction proved to be a very difficult item to vary in the course of these tests. In addition, some phenomena were observed that were atypical of the usual full-scale performance of icebreakers, for example, extensive crushing along the side of the hull. In spite of these problems it can be seen from Fig. 9 that the results obtained when the friction values measured during the tests are used agree quite favorably with the results collected during the full-scale trials. The increase with velocity, however, seems to be greater than that given by the regression of the full-scale data. This may be due to an additional viscous component of

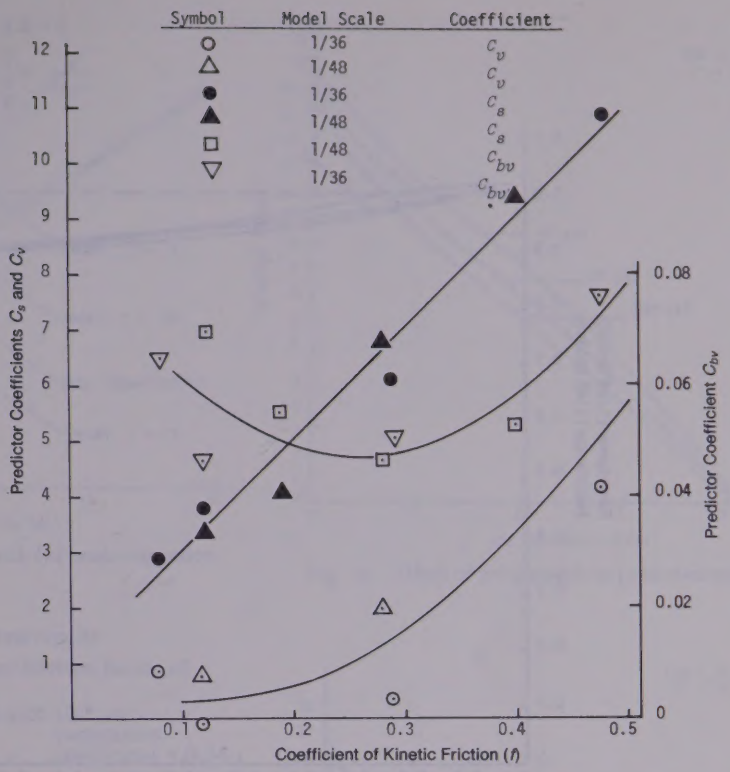

Fig. 6 Variation of regression coefficients with friction

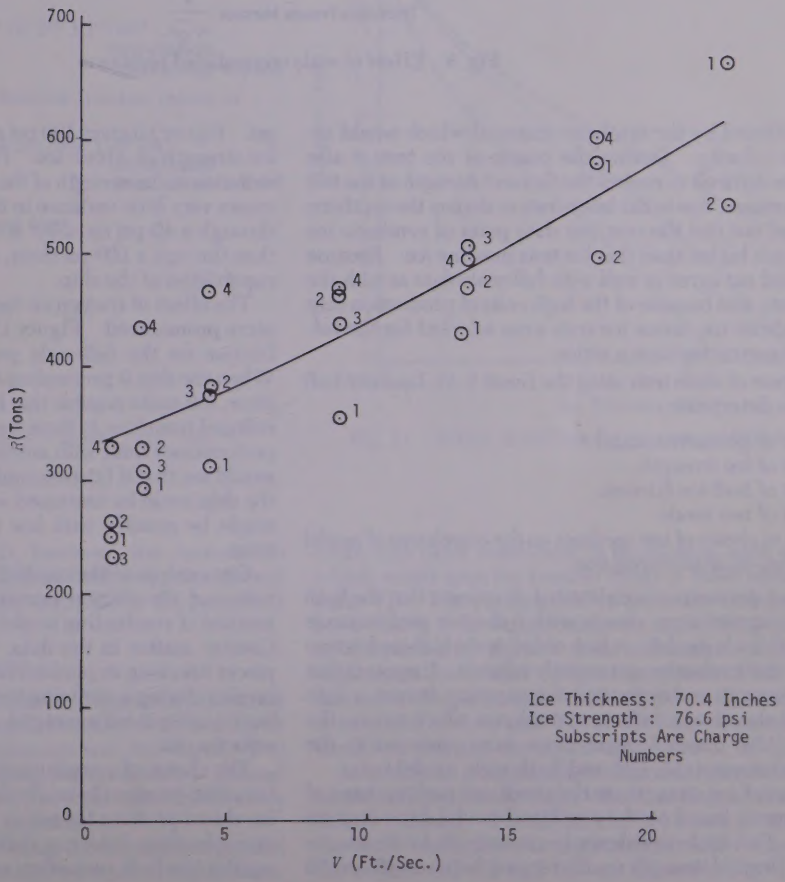

Fig. 7 Ramming tests in saline ice

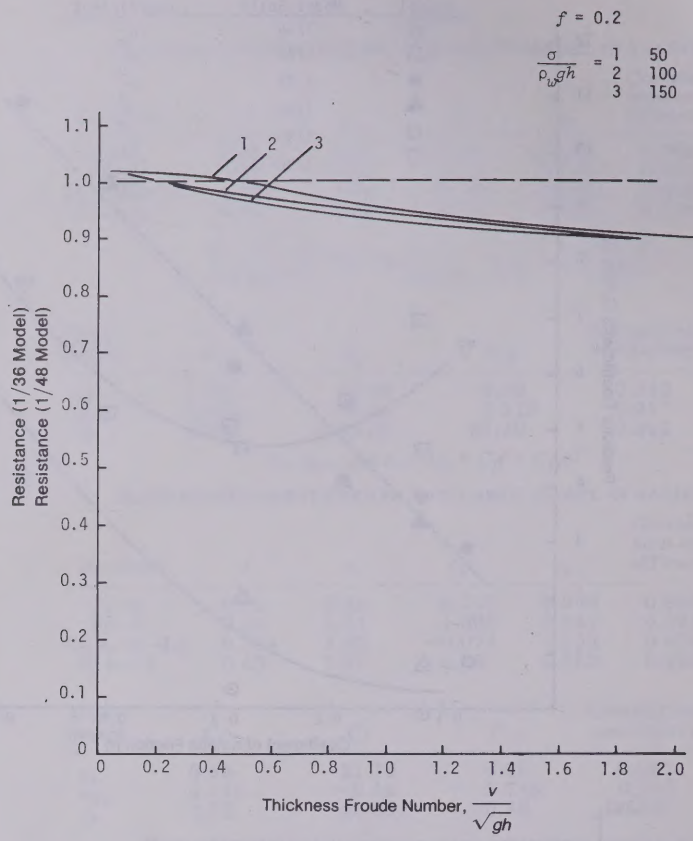

Fig. 8 Effect of scale on predicted resistance

resistance offered by the synthetic material which would increase with velocity. During the course of the tests it also proved quite difficult to control the flexural strength of the test ice. Furthermore, due to the labor costs to deploy the synthetic ice, it turned out that the cost/per data point of synthetic ice tests was much higher than that for tests in saline ice. Because the results did not agree as well with full-scale data as with the saline ice tests, and because of the high costs of production ship tests in synthetic ice, saline ice tests were selected for the following parametric resistance series.

The purpose of these tests using the *Louis S. St. Laurent* hull form was to determine:

- Effect of geometric scale.
- Effect of ice strength.
- Effect of hull-ice friction.
- Effect of test mode.
- Effect of choice of test medium on the correlation of model tests with full-scale performance.

Of the two geometric models tested, it appears that the 1/36th scale model agrees more closely with full-scale performance than the 1/48th scale model. A lack of full-scale hull-ice friction data makes that evaluation not entirely reliable. It appears that for tests of concepts and evaluation of competing designs, a 1/48th scale model also gives satisfactory results on which to base the evaluation. No unusual phenomena were observed in the differences between the 1/36th and 1/48th scale model tests.

The effect of ice strength on the predictor performance of the *St. Laurent*, based on the combined model data, is given in Fig. 10. Full-scale cantilever beam tests on Arctic sea ice have given flexural strength results varying between 40 and 70 psi. Figure 10 gives 100 psi as a conservative limit for flexural ice strength of Arctic ice. From this graph it is evident that variation in the strength of the ice encountered by an icebreaker causes very little variance in the performance and that progress through a 40-psi ice sheet is only approximately 1 knot faster than through a 100-psi sheet, even at the limiting performance capabilities of the ship.

The effect of friction on the performance of the ship is much more pronounced. Figure 11 is an illustration of the effect of friction on the full-scale performance of the *St. Laurent*. When the ship is proceeding through ice cover with sticky wet snow, it is quite possible that her maximum capability could be reduced from four to three feet. If we were to take 3½ ft as the performance limit with normal bare steel against clean ice, we would see that if friction could be reduced by 0.1 the speed of the ship could be increased well over a knot and a half. This might be possible with low friction coatings or bubbler systems.

Our analysis of the results from the constant-velocity towing tests and the inertial ramming tests indicates that the best method of conducting model tests is constant-velocity towing. Greater scatter in the data, which occurs due to individual pieces breaking in random fashion around the bow of the icebreaker during a ramming test, makes that method impractical. Such scatter is not averaged out as it would be for a constant-velocity test.

The choice of a medium still seems to indicate a preference for saline ice over the newly developed synthetic ice. Synthetic ice shows promise for use in certain types of model tests, for example, those involving deflection of ice, or impact of the ice against the hull, propeller, and appendages. For predicting

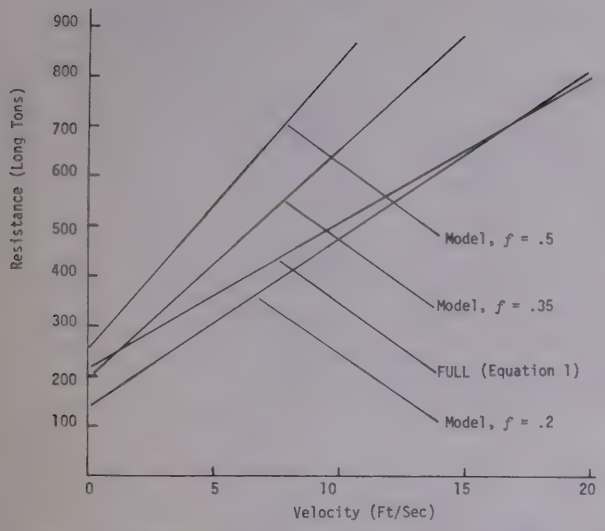

Fig. 9 Synthetic ice tests compared with full-scale regression

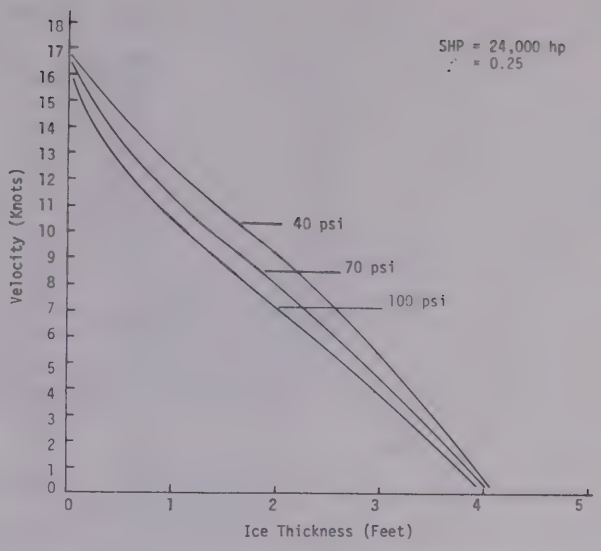

Fig. 10 Effect of ice strength on predicted resistance

Table 4 Synthetic ice test results

From the 1/36th model with a hull-ice friction factor of 0.51

$$R = 186.48 + 0.071 \cdot 10^{-3}\, \sigma_f h^2 + 26.933 \cdot 10^{-3}\, vh^2$$

correlation coefficient = 0.94

From the 1/48th model with a hull-ice friction factor of 0.16

$$R = 68.55 + 4.07 \cdot 10^{-3}\, \sigma_f h^2 + 13.27 \cdot 10^{-3}\, vh^2$$

correlation coefficient = 0.93

From the 1/48th model with a hull-ice friction factor of 0.51

$$R = 233.37 + .163 \cdot 10^{-3}\, \sigma_f h^2 + 25.469 \cdot 10^{-3}\, vh^2$$

correlation coefficient = 0.98

where
R = icebreaking resistance, long tons
σ = ice flexural strength, psi
v = ship velocity, fps
h = ice thickness, in.

$$R = C_0 + C_\sigma \sigma h^2 + C_v v h^2$$

with
$C_0 = a_0 + b_0 f$
$C_\sigma = a_\sigma + b_\sigma f$
$C_v + a_v + b_v f$
where f = hull-ice friction

$$R = (-6.80 + 470.92\, f) + (0.518 - 0.695\, f)10^{-3}\sigma h^2 + (7.703 + 34.835\, f)10^{-3} v h^2$$

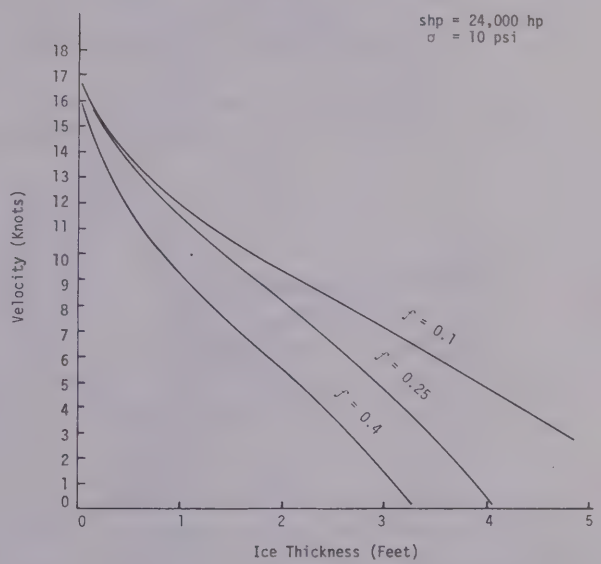

Fig. 11 Effect of hull-ice friction on predicted resistance

resistance with ship model tests, however, the necessity to control friction, control ice strength, and collect great numbers of data points at minimal expense requires, for the present at least, saline ice.

Parametric ice resistance tests

In the Introduction, the requirement to quantitatively assess the influence of variations in length, breadth, draft, and block coefficient on icebreaker performance was developed. For the purpose of these tests, icebreaking performance was defined as resistance offered to motion of the icebreaker by level ice (that is, continuous icebreaking resistance).

A series of seven different icebreaker models and two parallel mid-bodies was designed and constructed to vary length, beam, draft, and block coefficient in three steps, each over a range which would span the feasible range of these variables for the *Polar VII*. The center model in the beam-and-draft series has been chosen to have approximately scaled dimensions to those now expected for the new polar icebreaker. Table 5 lists the dimensions and model designation system of the models employed in the parametric tests. Table 6 shows the expected dimensions of the *Polar VII* at the time of the test program, Model B2-H2, and the scaled-up version of B2-H2.

As nearly as possible, each individual parameter has been varied independently of the others, with good design practice closely followed. For all but the two block variation models, the block coefficient was maintained at 0.56. Lines for two of the models (B2-H2 and H3) are shown in Fig. 12. The ap-

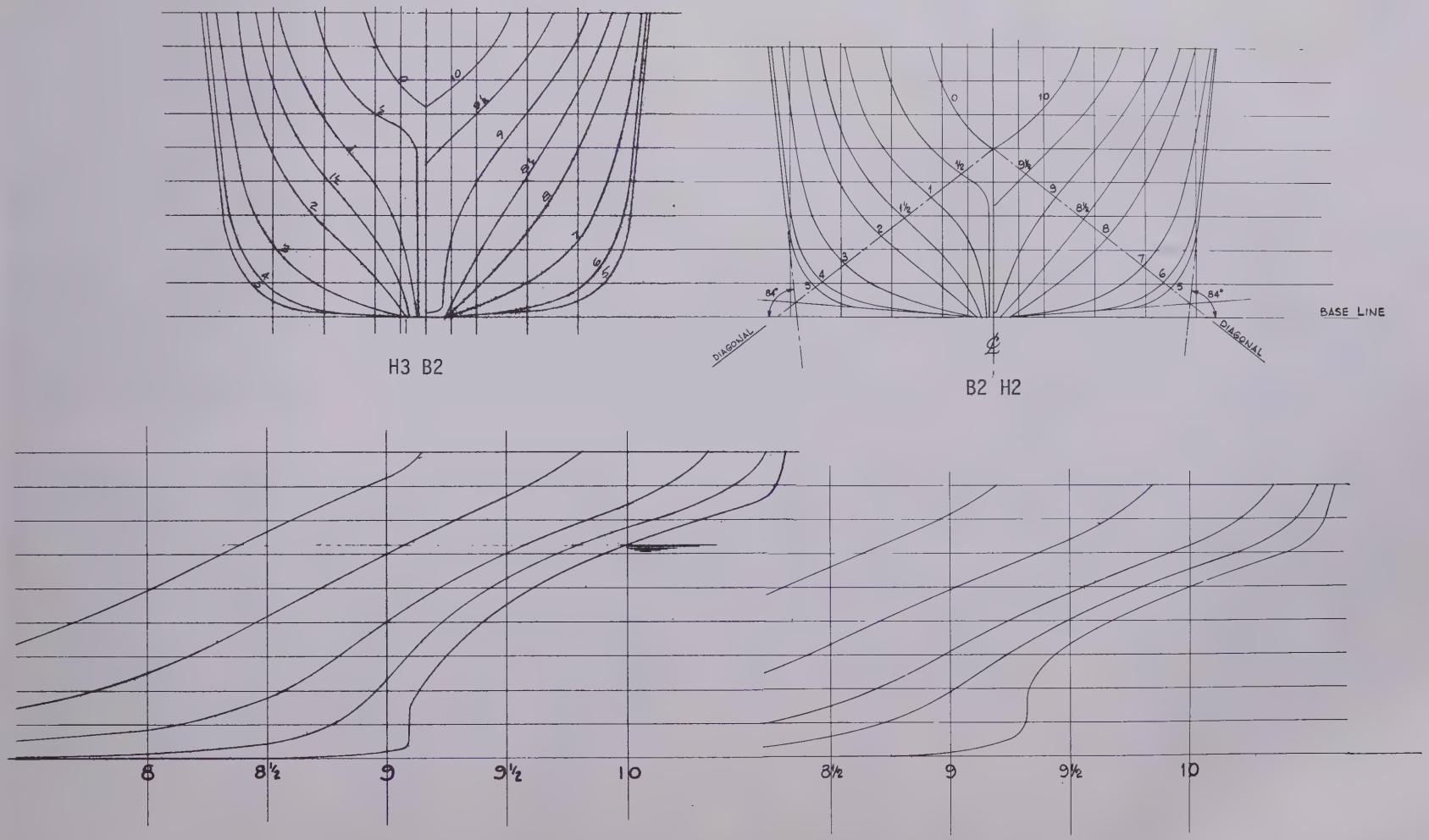

Fig. 12 Models lines for two hulls in the draft series

Table 5 Characteristics of parametric resistance test models

Model[a]	Length, cm	Beam, cm	Draft, cm	Block coefficient	Scale	Friction coefficient
H1,B2,L1,C2	239.2	42.8	13.9	0.56	71.3	0.208
B2,*H2*,L1,C2	239.2	42.8	16.9	0.56	71.3	0.190
H3,B2,L1,C2	239.2	42.8	20.3	0.56	71.3	0.213
C1,B3,H2,L1	239.2	53.4	16.9	0.50	71.3	0.238
C2,*B3*,*L1*,H2	239.2	53.4	16.9	0.56	71.3	0.245
C3,B3,H2,L1	239.2	53.4	16.9	0.625	71.3	0.245
B1,H2,L1,C2	239.2	37.4	16.9	0.56	71.3	0.228
L2,B3,H2,C2′	287.0	53.4	16.9	—[b]	71.3	0.230
L3,B3,H2,C2′	334.5	53.4	16.9	—[b]	71.3	0.230

[a] The models are referred to in the test by the italicized part of the model designator. It indicates the main parameter for which the effect on resistance was sought.

[b] For the purpose of the regression analysis, the block coefficient of these models was assumed unchanged by the addition of length.

Table 6

Designation	Displacement, tons	Length *BP*, m	Beam, m	Draft, m	Block coefficient	Scale
Polar VII[a]	33,000	173.0	30.5	12.2	0.5	full
B2-H2	32,100 (FW)	170.5	30.5	12.04	0.56	full
B2-H2	0.09689	2.392	0.428	0.169	0.56	model $\lambda = 71.3$

[a] Preliminary design dimensions at start of parametric ice resistance study.

Table 7 Parametric study model characteristics

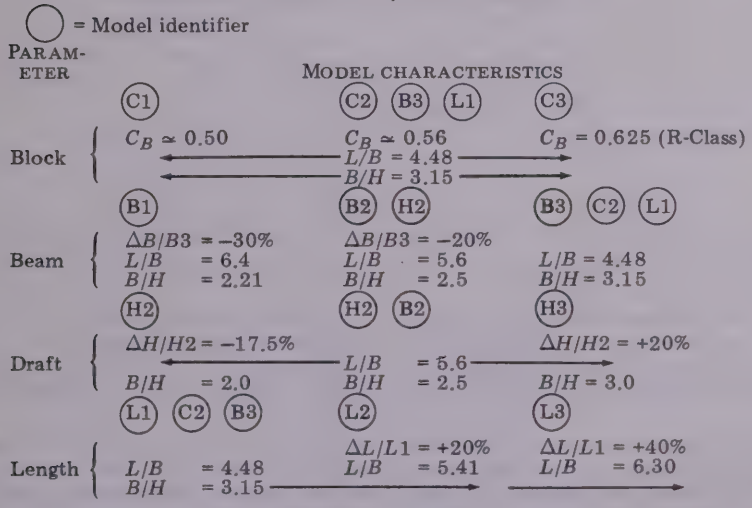

proach to maintaining block coefficient has been to maintain the same shape curve for sectional areas. The high-block ship is the original design for the R-Class icebreaker. The low- and middle-block ships have approximately identical midship section coefficients to the R-Class hull with finer lines fore and aft. Of course, addition of parallel middlebody for the length series results in higher blocks also. Table 7 shows the relationship of the parametric models to each other.

Results

The models were tested in saline ice at the ARCTEC ice model test facility in Columbia, Maryland. The test procedures and facility have been described previously to the Society.

All tests were conducted with two models towed simultaneously. The model surfaces were prepared, insofar as possible, in an identical way to produce similar values of hull-ice friction factors for all models. Although we were not entirely successful, the resulting values given in Table 5 do not exhibit large variation. The average friction coefficient was 0.23 with a maximum deviation from the average of 0.04. Later in the regression analysis of the data, we found that the effect of these small variations in friction factor was barely detected.

One hundred and ninety-six data points were acquired in level ice, the thickness of which was varied between 0.73 and 3.6 cm at model scale. The full-scale range for a geometric scale factor of 71.3, was 1.71 ft (0.52 m) to 8.4 ft (2.56 m). The

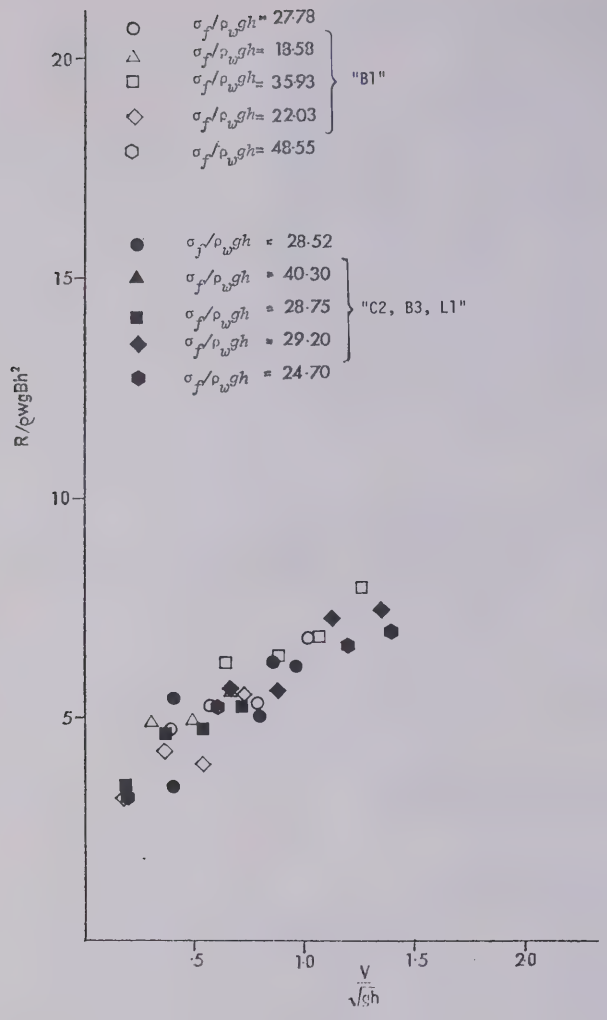

Fig. 13 Dimensionless resistance versus Froude number for model "B1" and "C2, B3, L1"

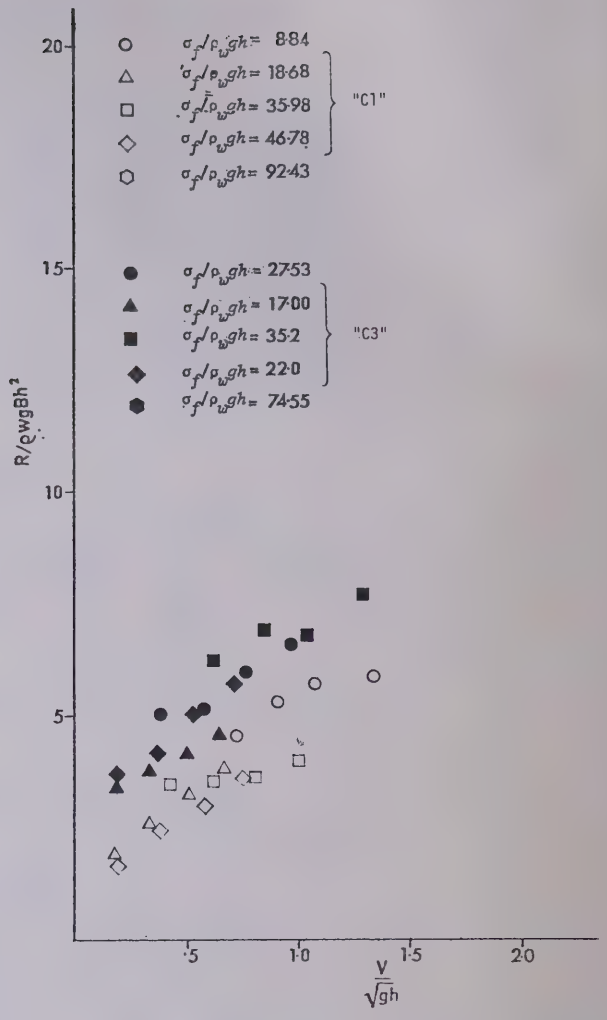

Fig. 14 Dimensionless resistance versus Froude number for model "C1" and "C3"

model ice strength was varied between 0.016 kg/cm^2 and 0.1 kg/cm^2. The full-scale range was 16.2 psi (1.13 kg/cm^2) to 111 psi (7.83 Kg/cm^2). The maximum model test speed was 70 cm/sec, corresponding to a full-scale ship speed of 11.5 knots (5.9 m/sec).

Measurements of ship resistance, ship speed, ice thickness, flexural ice strength, and elastic modulus were made for each test. The results are tabulated in Tables 26 through 37 in the Appendix. The dimensionless numbers $R/\rho_w gBh^2$, $v/\sqrt{gh}$, and $\sigma_f/\rho_w gh$ were computed for each test and are tabulated with the raw data in the Appendix.

The results of selected series of tests have been plotted in dimensionless form in Figs. 13–16. Figure 13 is a plot of $R/\rho_w gBh^2$ versus $v/\sqrt{gh}$ for the models with the largest and smallest beams. No difference between the two sets of data could be detected visually because beam was already included in the plot $R/\rho_w gBh^2$. Figure 14 is a similar plot for the models with the extreme values of block coefficient. In this plot it can be seen readily that the dimensionless resistance of the hull with a block coefficient of 0.625 is greater than that for the hull with a block coefficient of 0.5.

Figure 15 is a similar plot for the models with extreme values of draft. A distinct augmentation of dimensionless resistance is caused by increasing the draft from 13.9 to 20.3 cm or by 46 percent. Figure 16 is a similar plot for the models with extreme values of length. It is difficult to detect, by visual inspection, any length effect on resistance despite a 40 percent increase in length.

The test data were subjected to stepwise multiple regression analysis. In order for a variable to be accepted in the regression equation, its entry into the equation had to produce a reduction in the sum of the squares of the deviation from the regression which was significant at the 95 percent confidence level.

All terms containing ship length were rejected, and the following equation was derived:

$$\frac{R}{\rho_w gBh^2} = 5.7 + 0.147\frac{H}{h} - 7.83\,C_B{}^2 + \frac{\sigma}{\rho_w gh}(-0.318 + 0.265f + 0.394\,C_B) + \frac{v}{\sqrt{gh}}\left(-68.16 + 0.0477\frac{\sigma}{\rho_w gh} + 223.73\,C_B - 181.3\,C^2{}_B + 0.249\frac{H}{h}\right) \quad (2)$$

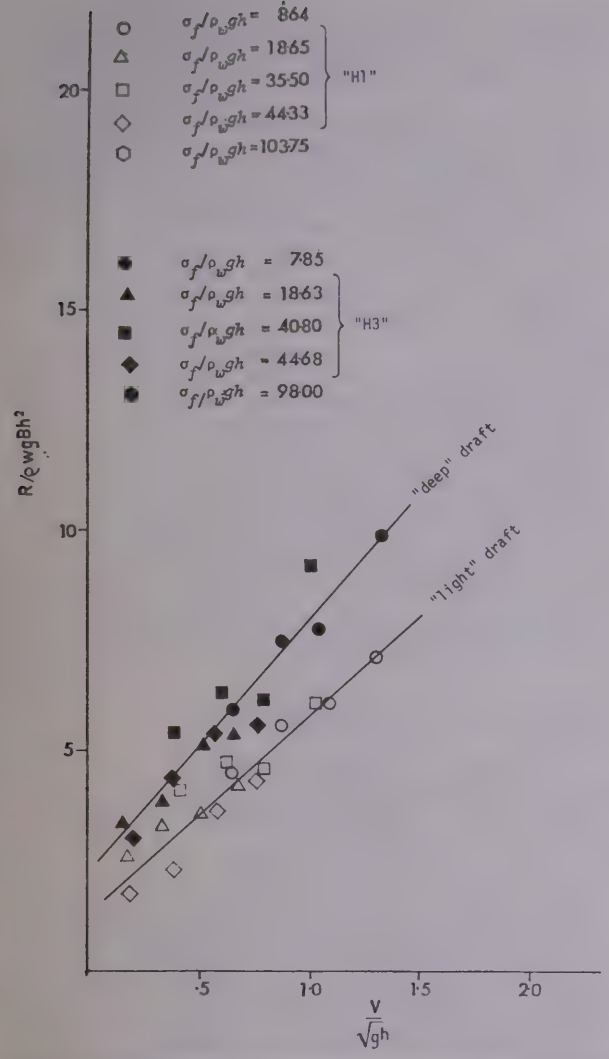

Fig. 15 Dimensionless resistance versus Froude number for model "H1" and "H3"

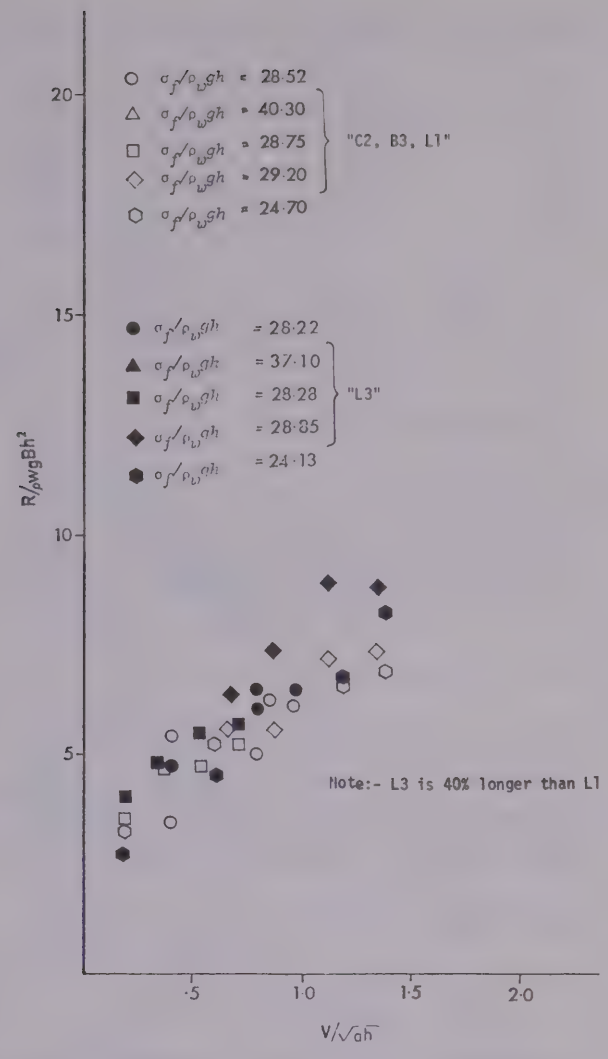

Fig. 16 Dimensionless resistance versus Froude number for models "C2, B3, L1" and "L3"

Nomenclature

B = ship's beam
L = length
C_B = block coefficient
R = turning radius
m = ship mass
x_G = distance of center of gravity from midship
A_f = rudder projected area
a = rudder aspect ratio
x_f = distance of rudder center of pressure from midship
δ = rudder deflection angle
λ = scale ratio
h = ice thickness
σ_f = flexural strength of ice
ρ_i = density of ice
ρ_w or ρ = density of water
g = gravity constant
Y_v = lateral force derivative coefficient
N_v = moment derivative coefficient
Y_r = rotary force derivative coefficient
N_r = rotary moment derivative coefficient
$Y_{v'}, N_{v'}, Y_{r'}, N_{r'}$ = nondimensional hull derivative coefficients as explained in Appendix 1
β = ship drift angle
u = forward velocity component
v = transverse velocity component
V = ship speed or towing speed
r = yaw angular velocity
l = rotating arm length
Y_δ = rudder force derivative coefficient
N_δ = rudder moment derivative coefficient
$(Y_v)_f, (N_v)_f$ = derivative coefficient for control fins, that is, rudder
$(Y_v)_s, (N_v)_s$ = derivative coefficient for step
$(Y_v)_{fs}, (N_v)_{fs}$ = derivative coefficient for rudder and step
C_L = rudder lift coefficient
C = stability criteria
C' = nondimensional stability criteria
X = ship's longitudinal forces
Y = ship's lateral forces
N = ship's moment

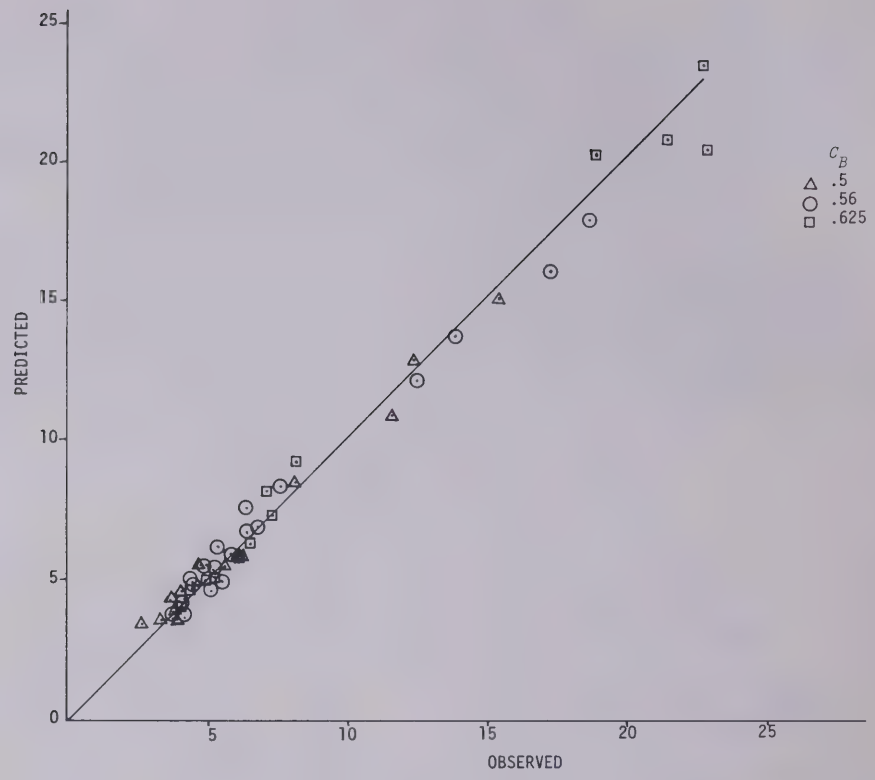

Fig. 17(*a*) $R/\rho_w gBH^2$ predicted versus $R/\rho_w gBH^2$ observed

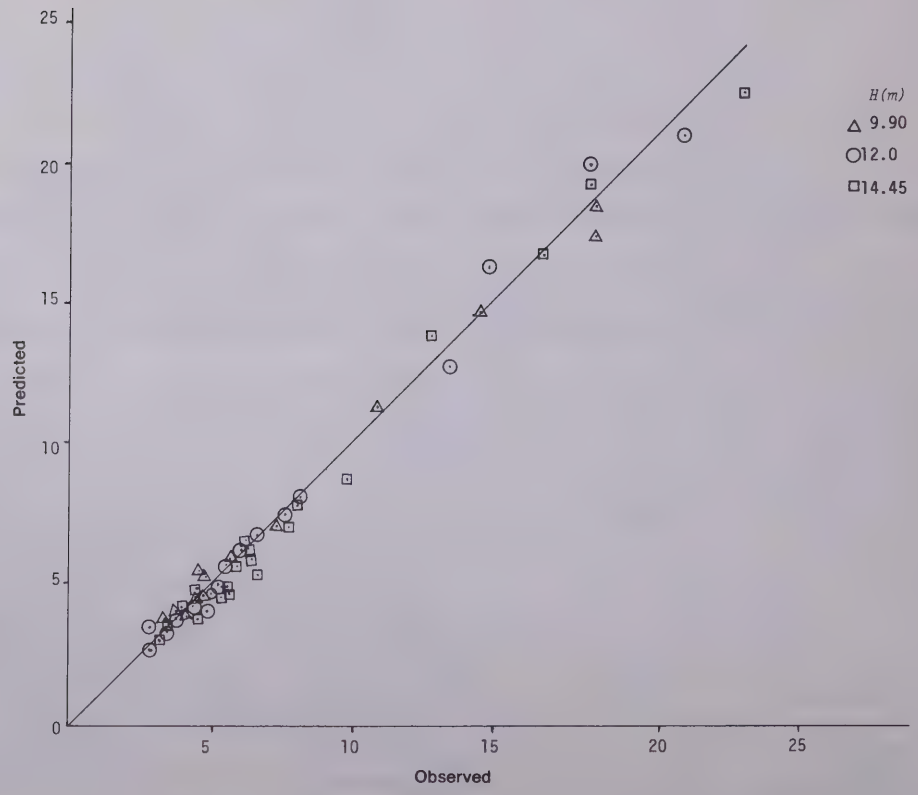

Fig. 17(*b*) $R/\rho_w gBH^2$ predicted versus $R/\rho_w gBh^2$ observed

Equation (2) equates dimensionless resistance to combinations of dimensionless strength $\sigma/\rho_w gh$, dimensionless velocity $v/\sqrt{gh}$, block coefficient C_B, draft-to-thickness ratio H/h, and hull ice friction factor f.

Equation (2) cannot be guaranteed as the best fit to the data because we simply could not include all of the permutations and combinations of the various variables, particularly at higher orders, in the stepwise regression analysis. However, of the variables considered which could have been selected by regression analysis, the ones shown are the significant ones at the 95 percent confidence level.

The multiple correlation coefficient for this regression was 0.9914, with a standard error of 0.696 or 8.8 percent of the mean value of dimensionless resistance.

To demonstrate graphically the degree to which equation (2) fits the data, the predicted values of dimensionless resistance $R/\rho_w gBh^2$ have been plotted against the observed values in Fig. 17(*a*) for the C_B variation tests and in Fig. 17(*b*) for the draft variation tests. It is important to note that the values predicted by the regression equation are not biased with respect to the observed values for any of the different models; that is, data points for a particular block model or draft model are not asymmetrically distributed about the 45 deg line plotted in the figures.

Equation (2) is valid only over the range of independent variables for which tests were made, as shown in the following:

$$104 > \frac{\sigma}{\rho_w gh} > 8 \tag{3}$$

$$2.5 > \frac{v}{\sqrt{gh}} > 0.2 \tag{4}$$

$$0.625 > C_B > 0.50 \tag{5}$$

$$73.0 > \frac{H}{h} > 10 \tag{6}$$

Equation (2) indicates that, for the range of variables tested, level ice resistance is a linear function of beam. Exercising the equation for a reasonable range of full-scale ice strength demonstrated that the influence of ice strength was virtually insignificant. The equation indicates that level ice resistance for the type of ship tested is influenced significantly by draft and block variations.

Table 8 illustrates the effects of variations in block coefficient and draft on resistance in 7 ft (2.13 m) of ice at 3 knots (1.54 m/sec) with an ice strength of 80 psi (5.6 kg/cm^2) for a ship with a beam of 98.4 ft (30 m).

A subroutine was developed which solved equation (2) for ice thickness for given values of propulsive thrust, speed of advance, ship breadth, draft and block coefficient, ice strength, and hull-ice friction factor. This subroutine formed one of the main constraints in the Icebreaker Feasibility Design Model, which is described in a later section of this paper.

Table 8 Effect of draft and block coefficient variations on resistance

C_B	Draft 32.5 ft (9.90 m)	Draft 31.45 ft (12.03 m)	Draft 47.4 ft (14.45 m)
0.50	445[a]	476	512
0.56	551	583	619
0.625	589	620	656

[a] Numbers are the values of resistance, in tons, for the following conditions:

Beam	30 m	(98.4 ft)
Speed	1.5 m/sec	(3 knots)
Ice thickness	2.13 m	(7 ft)
Ice strength	5.6 kg/cm^2	(80 psi)
Hull ice friction factor	0.25	

Maneuverability program

Good maneuvering and coursekeeping qualities are recognized as being important requirements for icebreaking ships as well as for ordinary surface ships. Icebreakers particularly require high maneuverability for rescue and escort operations.

Techniques and theories for predicting the important characteristics of maneuvering and coursekeeping ability for ordinary surface ships have been perfected to a satisfactory level, but unfortunately very little effort has been exerted to understanding these characteristics for icebreaking ships. The first significant full-scale turning tests were conducted on the CCGS *Labrador* in sea ice during the winter of 1973, and thus provided the first full-scale data for the model and full-scale correlation study [13].

The objectives defined in the scope of the maneuvering program were first to validate the correlation between the model test results and Labrador full-scale turning tests and, second, upon the validation of the model testing technique, to determine the effects of block coefficient and ship length on the turning radius and directional stability. In order to accomplish these objectives, a method of determining the maneuverability and directional stability was devised.

Development of an icebreaking maneuverability model test technique

One of the measures of maneuverability of a ship is the turning circle diameter. As the turning circle becomes smaller, a ship is said to become more maneuverable; that is, a ship can change its course more promptly with rudder movement. As such, the turning circle diameter of a ship appears to be the most direct measure of the maneuverability, and was selected in this program.

The turning circle radius of a ship can be found using the linear theory of ship motion which has been well developed in the past [14]. This is given by

$$\frac{R}{L} = \frac{Y'_v(N'_r - m'x'_G) - N'_v(Y'_r - m')}{Y'_v N'_\delta - N'_v Y'_\delta}\frac{1}{\delta} \tag{7}$$

In order to determine the turning radius, the hull force and moment derivatives (Y'_v, N'_v, Y'_r, N'_r) and the rudder force and moment derivatives ($Y'\delta$, $N'\delta$) must be determined. These hull derivatives can be found experimentally and the rudder force and moment derivatives estimated theoretically.

If a ship can maintain a straight-line course without rudder action after a small disturbance (such as a disturbance caused by a nonuniform ice condition, wind, or current), she is said to be directionally stable and has good coursekeeping ability. In order to maintain a straight-line course, the yaw-and-sway velocity of the ship must be zero sometime after the disturbance. Whether the yaw-and-sway velocity becomes zero can be determined from the stability criteria derived from the same theory, and as given by

$$C' = Y'_v\,(N'_r - m'x'_G) - N'_v\,(Y'_r - m') > 0 \tag{8}$$

This stability criterion can be computed with the hull force and moment derivatives determined experimentally.

Design of an economical modeling system. Several experimental methods can be employed to determine maneuvering characteristics in level ice. The free-running model test is one of these methods and can be used for a given specific rudder design to determine the characteristics of a specified maneuver during the tests. This test requires a large maneuvering basin, and model tests have to be conducted in different ice thicknesses with different rudder angle; consequently, the

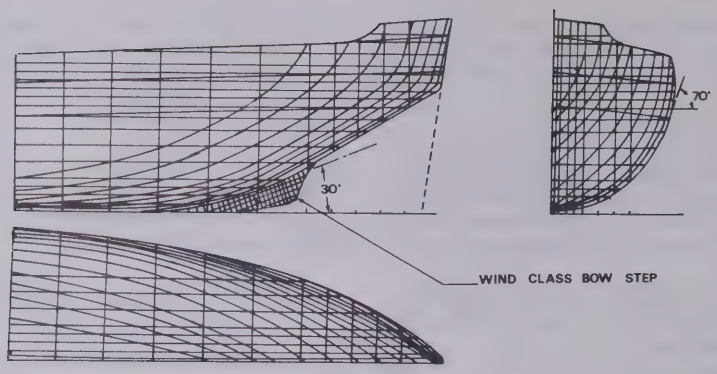

	WIND	LABRADOR
Scale Ratio (λ)	1:36	
Length W.L. (ft)	6.94	250.
Beam (ft)	1.72	62
Draft (ft)	0.72	25.75
Block Coefficient	0.47	0.47
Displacement (lbs)	252.5	5360 L. Tons
Friction Factor	0.28	

Fig. 18 Lines of *Labrador* and *Wind* model with step

test is very expensive. Other indirect experimental methods provide the information on hull force and moment derivatives and are more versatile to apply to the prediction of maneuvering performance. Among these, the planar motion mechanism, oscillator, and rotating arm methods were considered. Although the test results obtained using the planar motion mechanism (PMM) can provide the most complete information on the hull force and moment derivatives, the construction of a PMM system suitable for ice tests, and the reduction of the data obtained during the PMM tests in ice, was expected to be very complex and costly. In addition, the statistical time-varying nature of icebreaking forces would complicate analysis of such tests where turning rate is constantly varying. For the same reason, oscillation techniques were also ruled out. Consequently, the rotating arm test method was adopted where a ship model is towed along a segment of a circle.

Two different types of tests were devised; one was a straight-line test and the other a rotating test. In the straight-line tests the models were towed at constant velocity along a straight line parallel to the basin with a drift angle varying between −3 and 12 deg. This straight-line towing of a model with a drift angle generated a transverse velocity component and thus provided the data to plot the forces and moments against the transverse speeds. The distance of travel for each run was about two ship lengths. In the rotating tests, the models were towed along an arc segment by the rotating arm. This rotation generated a pure yaw angular velocity in the model. The rotating tests thus provided the data to plot the longitudinal forces and moments versus the yaw angular velocity. The lengths of the arc segment tests were 15.4, 12.2, and 9.6 ft, respectively (4.7, 3.7, and 2.9 m).

Full-scale/model-scale correlation. *Labrador* full-scale turning tests were conducted south of Lowther Island on October 27, 1973 [13]. The ice on the turning course was an average 11 to 12 in. (28 to 30 cm) thick with a slight pressure noticed in some places. The ice strength measured during these tests was 4.8 kg/cm^2 (68 psi). The tests were run with full power (approximately 8300 shp) with the rudder hard over, that is, a 37.5-deg rudder angle. The positions of the vessel during the turning tests were obtained accurately with a two-station hydrodist system. Two turning paths were thus obtained, one right-hand and one left-hand turn.

An existing 1/36th-scale *Wind*-Class model was selected as a substitute for a *Labrador* model for the full-scale/model-scale correlation program. The two ships have exactly the same hull forms except that the step in the bow is not present on *Labrador*. The lines drawings and principal dimensions of a *Wind*-Class icebreaker on which the model is based and of *Labrador* are given in Fig. 18. The tests were conducted without a rudder. The *Wind* model was towed at a full-scale equivalent 12.7 and 10.1 knots, respectively, in ice whose full-scale equivalent is 1 ft (30 cm). The strength of ice was maintained during the model tests at a level equivalent to 1/36th that observed at full scale. A summary of the model test data is given in the Appendix. The model test data were reduced and then nondimensionalized in a manner similar to that used for the analysis of continuous icebreaking towing test results, to allow direct comparison with full-scale test data and also to reduce the number of variables for analysis. An example of the data collected is given in Fig 19, which shows the rotary force versus yaw velocity in nondimensional terms. The dimensional version of the derivative coefficients (Y_v, Y_r, N_v, N_r) required to compute the turning radius and stability criteria was obtained by computing the slope of each force versus velocity curve at the origin and then multiplying by the appropriate distortion ratio. For example, to compute Y_v, the slope of $Y/\rho_w gBh^2$ versus $v/\sqrt{gh}$ was first evaluated at $v/\sqrt{gh}=0$. This slope was then multiplied by the distortion ratio $\rho_w gBh^2/\sqrt{gh}$ to produce Y_v. These are expressed in the following form:

$$Y_v = Y_v^* \frac{\rho_w gBh^2}{\sqrt{gh}} \text{ where } Y_v^* = \frac{Y}{\rho_w gBh^2} \Big/ \frac{v}{\sqrt{gh}} \tag{9}$$

$$N_v = N_v^* \frac{\rho_w gBLh^2}{\sqrt{gh}} \text{ where } N_v^* = \frac{N}{\rho_w gBLh^2} \Big/ \frac{v}{\sqrt{gh}} \tag{10}$$

$$Y_r = Y_r^* \frac{\rho_w gBh^2}{\sqrt{g/r}} \text{where } Y_r^* = \frac{Y}{\rho_w gBh^2} \Big/ \frac{r}{\sqrt{g/r}} \tag{11}$$

$$N_r = N_r^* \frac{\rho_w gBLh^2}{\sqrt{g/h}} \text{ where } N_r^* = \frac{N}{\rho_w gBLh^2} \Big/ \frac{r}{\sqrt{g/h}} \tag{12}$$

where Y_v^*, N_v^*, Y_r^*, and N_r^* are nondimensional force and moment slopes measured at origin from force versus velocity plots, and the multiplication factors appearing in the equations (9) through (16) are distortion ratios. These distortion ratios are computed from a given ship's beam, length, ice thickness, gravity constant, and water density. The values of these ratios are the same for both the model and for the full-scale ship.

The *Wind*-Class model was tested without the rudder. The effect of the rudder on the hull derivative coefficients was accounted for as was the effect of the step of the *Wind* model. It was assumed that these effects could be corrected for, using the theory developed for open-water tests [15]. The derivative coefficients for the step or the fixed rudder were found from relationships of the following form:

$$(Y_v)_f = -\frac{\rho}{2} A_f V \frac{\partial C_L}{\partial \beta} \tag{13}$$

$$(N_v)_f = (Y_v)_f \cdot x_f \tag{14}$$

$$(Y_r)_f = (N_v)_f \tag{15}$$

$$(N_r)_f = (Y_v)_f \cdot x_f \tag{16}$$

The combined derivative coefficients for the rudder and the step were then computed by adding algebraically the coefficients computed using equations (13) through (16), for both the rudder and step, to the experimentally derived coefficients in Table 9. The principal characteristics of the rudder and the step required for the computation of the derivative coefficients are given in Table 10. The computed derivative coefficients for the rudder step are given in Table 11. The hull derivative coefficients corrected for the effect of the rudder and the step are listed in Table 12.

The rudder deflection force and moment derivative coefficients were computed as follows:

$$Y_\delta = \frac{\rho}{2} A_f V \frac{\delta C_L}{\delta B} \tag{17}$$

$$N_\delta = -Y_\delta \cdot x_f \tag{18}$$

where V is the flow velocity at the rudder.

Using the value of ship speed for V, the rudder force derivative (Y_δ) was reduced by a factor of 0.65 to account for the wake and race effects on a counterline rudder between twin screws [16].

The corrected model derivative coefficients from Table 12 and the corrected rudder force and moment derivatives from equations (17) and (18) were inserted into equation (7) to compute turning radius per unit ship length.

The turning circles predicted from the model test results are shown in Fig. 20 compared with the full-scale turning circle. The full-scale turning radius obtained graphically for the right-hand turn varied between 790 and 1164 ft. The predicted turning radius is on the other hand, 820 ft, and this lies well within the range of the measured turning radius. As for the left-hand turn, the predicted turning radius is 685 ft and the measured turning radius ranges between 275 and 993 ft. Again, the predicted turning radius is well within that range. In order to look at this result from a different aspect, the turning radius per ship length of the model prediction and for the full-scale tests is plotted against the approach speed in Fig. 21. The fair agreement exhibited between the model predictions and the *Labrador* full-scale test results prompted the undertaking of the parametric maneuvering tests using these simulation techniques.

Parametric model tests

For the parametric model tests, three of the models tested in the parametric resistance test program were used to determine the effects of hull form on icebreaking resistance. These were the "C2, B3, L1" model, the "C3" model, and the "L2" model. These three models are designated Model 1, Model 2, and Model 3 in this section. Models No. 1 and No. 2 are block coefficient series models and Models No. 1 and No. 3 are length variation models. These models were tested together with the rudders fixed on the centerline. If Model No. 2 is scaled up using a scale ratio of 36, the full-scale ship becomes an R-Class icebreaker. At a scale ratio of 72, Model 1 simulates an icebreaker similar to *Polar VII*. Therefore, for the parametric model tests, a scale ratio of 72 was selected for the model properties and model towing speeds. Models 1, 2, and 3 were towed to a model speed equivalent to a full-scale speed of 6 knots through model (saline) ice fields of a thickness equivalent to a full-scale thickness of 3 ft (91 cm). In order to determine the effect of ice thickness on turning radius, Model 1 was towed through a model ice field equivalent to a full-scale thickness of 6 ft (183 cm) at a full-scale velocity of 3 knots. A summary of the model test data is included in the Appendix. Plots of nondimensional sway force and rotary moments versus nondimensional sway and yaw velocity were then used to develop dimensionless derivatives in a manner identical to that previously described for the *Labrador* model tests. The dimensional hull derivative coefficients were then calculated by multiplying by the distortion factor based on the desired ice thickness.

Since the parametric models were tested with the rudder, the effect of the rudder on the hull derivative coefficients is already included. The dimensional hull derivative coefficients for the parametric models are listed in Table 13. The units of deriv-

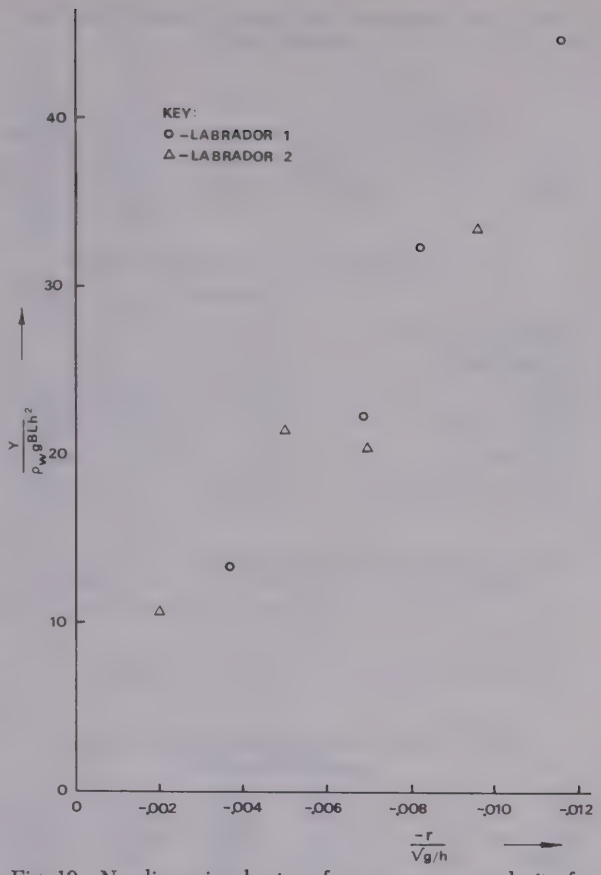

Fig. 19 Nondimensional rotary force versus yaw velocity for *Wind* model

Table 9 Hull derivative coefficients for *Wind*-Class model (uncorrected)

	v (knots) Approach speed	Y_v lb / fps	N_v ft-lb / fps	Y_r lb / rad/sec	N_r ft-lb / rad/sec
Labrador	12.7	−0.135	−4.90	−4.09	−578.1
Labrador	10.1	−0.141	−3.92	−4.09	−412.9

Table 10 Model rudder and step dimensions

	Rudder	Step
Rudder dimension (chord × span, ft)	0.42 × 0.28	
Projected area, sq ft	0.12	0.09
Aspect ratio, a	1.50	0.05*
Lift curve slope $(\frac{\delta C_L}{\delta \beta})$**	2.36	1.66***
Distance from midship	$\frac{0.965\ L}{2}$	$\frac{0.86\ L}{2}$

*Ratio of step thickness to step depth.
**Obtained from Jones' formula [10]

$$\frac{\delta C_L}{\delta \beta} = \frac{\pi a}{2}$$

***From reference [15], p. 502, for a flat plate.

Table 11 Model hull derivative coefficients for rudder and step

Rudder	12.7	−0.0112	1.14	1.14	−116.7
Step	12.7	−0.0078	−0.66	−0.66	−55.8
Combined	12.7	−0.0034	1.80	1.80	−60.9
Rudder	10.1	−0.0089	0.90	0.90	−92.6
Step	10.1	−0.0062	−0.53	−0.53	−44.3
Combined	10.1	−0.0027	1.43	1.43	−48.3

Table 12 *Wind*-Class model derivative coefficients corrected to *Labrador*

Labrador	12.7	−0.138	−3.10	−2.29	−639.0
Labrador	10.1	−0.144	−2.49	−2.66	−461.9

ative coefficients are in feet, pounds, and seconds.

The rudder dimensions for the parametric models are given in Table 14.

Since the *Polar VII* will have triple screws with one rudder behind the center screw, the effects of wake and race were accounted for by using normal force ratios presented in [16] for a rudder behind a single screw.

Effect of block coefficient on turning radius

The test results of two models, which were identical except for the block coefficient, were compared to evaluate the effect of block coefficient on the turning radius. The turning radii of the two ship models predicted for a turn in a level ice field, 3 ft thick at a speed of 6 knots, are plotted in Fig. 22 versus the rudder deflection angle. The turning radius per unit length of the model with the lower block coefficient is about 3.3 and that of the model with the higher block coefficient about 6.3 at a rudder angle of 35 deg. The increase in the block coefficient from 0.555 to 0.625 has resulted in the increase in dimensionless turning radius of 95 percent. The reason for this significant increase in dimensionless turning radius seems to be that for the hull with the high block coefficient, the slope of the hull, as the midship section is approached, is more nearly vertical than that of the low block hull. Consequently the icebreaking forces and moments developed in a turn of a given radius will be higher for the high-block hull than for the low-block hull. Conversely, with similar available turning forces, the radius of the turn will be larger for the high-block hull form.

Effect of length variation on turning radius

Two models were tested which were different only as to length of parallel middlebody; one model was 20 percent longer than the other. The predicted turning radius per unit ship length of each of the two models is plotted versus rudder angle in Fig. 23 for an approach speed of 6 knots. As can be seen in the figure, the turning radius of the longer ship is significantly greater than that of the shorter model. The turning radius per unit ship length is 10.4 for the longer model and 3.0 for the shorter model at a rudder angle of 35 deg. *An increase in ship length of 20 percent caused an increase in turning radius per ship length of 300 percent. The absolute turning radius has increased by 366 percent as compared with that of the shorter model.* The stability criteria also indicate that the longer model is more directionally stable. A simplified explanation for this greater turning radius is that for a ship to turn in ice, the ship side must break ice. The longer model must break ice over a greater length than must the shorter model in a turn of equal radius. Hence, the tests predict much higher forces and moments for the longer ship to achieve the same radius turn, and, conversely, the ship will execute a much greater radius turn with the same available turning forces.

Model 1 was tested in two different ice thicknesses to compare the turning radius. For one test, the ice was 3 ft thick (full scale) and the approach speed was 6 knots. For the other test, the ice was 6 ft thick (full scale) and the approach speed was 3 knots. The ice strength was about 70 psi. The turning radius per ship length is 6 ft, and in 3-ft-thick ice is plotted in Fig. 24 versus the rudder deflection angle. As can be seen in the figure, the turning radius is greatly influenced by ice thickness. By increasing the ice thickness from 3 to 6 ft, the turning radius per ship length increased from 3.3 to 37.5 at a rudder angle of 35 deg. The turning radius in 6-ft-thick ice is 11 times greater than that in 3-ft-thick ice.

Pathkeeping ability and maneuverability of a ship can also be evaluated from the plot of yaw velocity versus rudder deflection angle. This curve indicates the heading angle change per unit time at a certain rudder angle. The yaw angular velocity for the parametric models is plotted in Fig. 25 versus the rudder angle. If the slope of the yaw angular velocity curve at zero rudder angle is negative, a ship is directionally stable. If this slope is positive, a ship is directionally unstable. The marginally stable ship would have an infinite slope.

Another method of determining the directional stability of a ship is to theoretically compute the stability criterion as described earlier. If this value is positive, a ship is directionally stable. The values of the stability criterion for each model for a rudder angle of 30 deg are listed in Table 15.

It can be concluded from these plots that all parametric models are directionally stable in ice. More specifically, ships of higher block coefficient are more stable than ships of lower block coefficient, and longer ships are more stable in level ice than shorter ships. All ships are generally more stable in thicker ice.

As for the maneuverability, the opposite is true; that is, lower block coefficient ships and shorter ships are more maneuverable in thick ice.

Therefore, as far as the hull form is concerned, better maneuverability and better coursekeeping ability create a conflict in designer-selected parameters. But better maneuverability

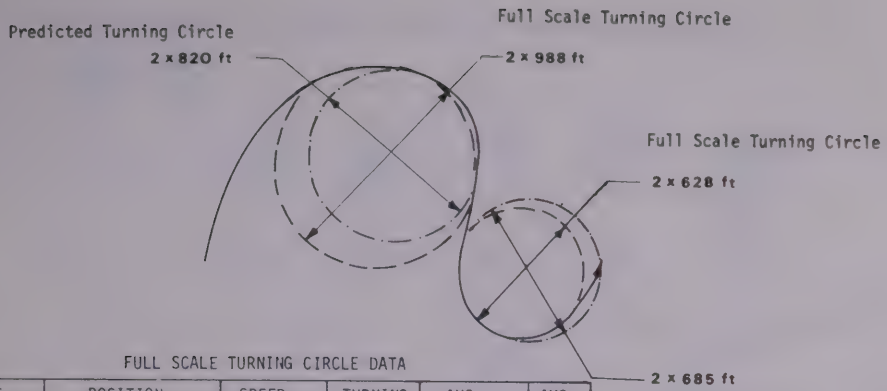

FULL SCALE TURNING CIRCLE DATA

TIME MIN.	POSITION X	POSITION Y	SPEED FT/SEC	TURNING RADIUS FT.	AVG. SPEED FT/SEC	AVG. RADIUS FT.
17.0	2178	3517	22.6	1164		
17.5	2915	3506	23.0	1009	21.44	988
18.0	3472	3034	22.3	790	12.7 knots	
19.5	3354	1308	27.23	615		
20.0	3626	986	26.02	275	17.02	628
20.5	4239	1046	27.80	993	10.07knots	

Fig. 20 *Labrador* trial turning circle and predicted turning circle

can be achieved if required by improving the rudder design, that is, by increasing the number of rudders, the rudder projected area, and by improving the hull form around the rudders.

Conclusions

The first objective of the icebreaking maneuvering program was to confirm the validity of the model maneuvering test techniques. This objective has been met in that the model prediction for the turning radius of *Labrador* was in satisfactory agreement with the *Labrador* full-scale turning circle data.

The second and third objectives of this model test program were to determine the effect of block coefficient and ship length on the ship maneuverability and coursekeeping ability. These objectives were met, and the following conclusions were reached:

- Block coefficient is a significant parameter in determining ship maneuverability in level ice. Increasing block coefficient (without change to other parameters) will produce greater turning radius in ice. More specifically, the turning radius per ship length increased from 3.3 to 6.3 by increasing the block coefficient from 0.555 to 0.625. Thus, higher-block ships are less maneuverable in ice.
- Ship length is an extremely important parameter for the maneuverability. The increase of ship length by 20 percent resulted in the increase of turning radius by 305 percent.
- Generally, ships are directionally stable while continuously moving through level ice. Longer ships and higher-block ships have more directional stability and thus better coursekeeping ability.
- Since this model maneuvering test technique has proved to be a sound means to evaluate the maneuverability and coursekeeping ability of a ship, it is recommended that model maneuvering tests be included in future ice model test programs to determine the maneuverability and coursekeeping ability of contemplated icebreaking ship designs.

Icebreaker Feasibility Design Model

The Icebreaker Feasibility Design Model is a computerized preliminary design tool. It is described in general by Melberg

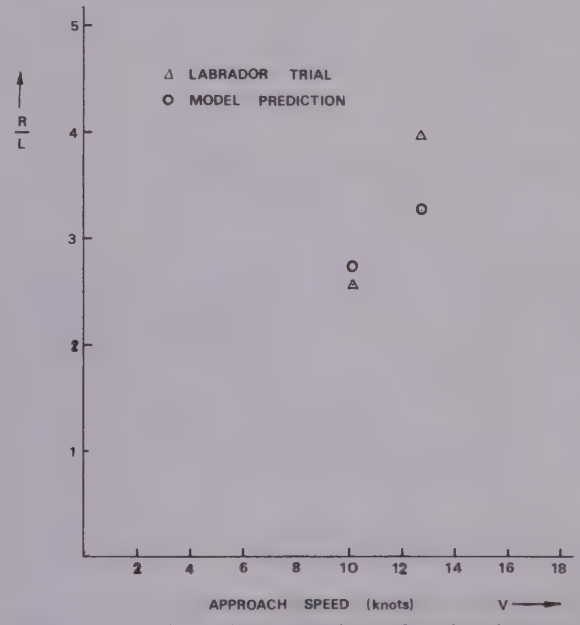

Fig. 21 *Labrador* trial turning radius and predicted turning radius

et al [1]. It is a simulation of the iterative process normally used by naval architects to produce a ship design with a given set of owners' requirements and constraints. Table 16 lists the owners' requirements which may be handled by the program. The program is started with a reasonable set of values for L/B, B/H, C_B, C_P, Δ, and SHP. Checks are made to determine whether that set can satisfy the owners' requirements. If they do, the cost of the ship is calculated. A random-number generating program then selects new values for one of the foregoing variables. The range of allowed values for the variables is shrunk exponentially as the program iterates, gradually converging upon a set of those values which simultaneously satisfies

Table 13 Dimensional hull derivative coefficients (full scale units)

	Y_v	N_v	Y_r	N_r	Ice thickness, ft	Approach speed, knots
Model 1	−0.485	−6.01	−5.57	−396.0	3	6
Model 2	−0.519	−6.01	−2.94	−573.9	3	6
Model 3	−0.858	−0.91	−12.08	−969.3	3	6
Model 1 in thick ice	−2.159	−17.00	−19.27	−2431.3	6	3

Table 14 Rudder dimensions for parametric models

	Model scale	Full scale
Rudder size (chord × span)	0.38 × 0.209 ft	27.4 × 15.0 ft
Projected area	0.079 sq ft	411.0 sq ft
Aspect ratio	1.81	1.81
$\frac{\partial C_L}{\partial \beta}$ (per radian)	2.75	2.75

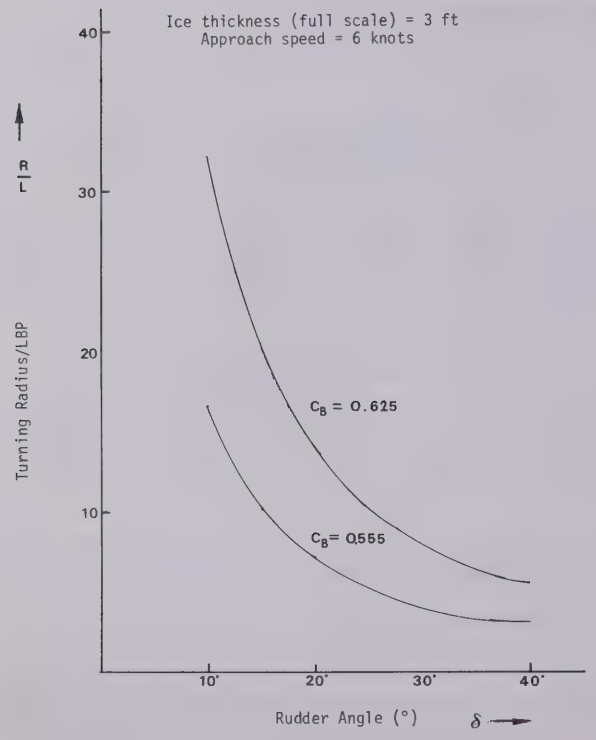

Fig. 22 Turning radius of block coefficient models

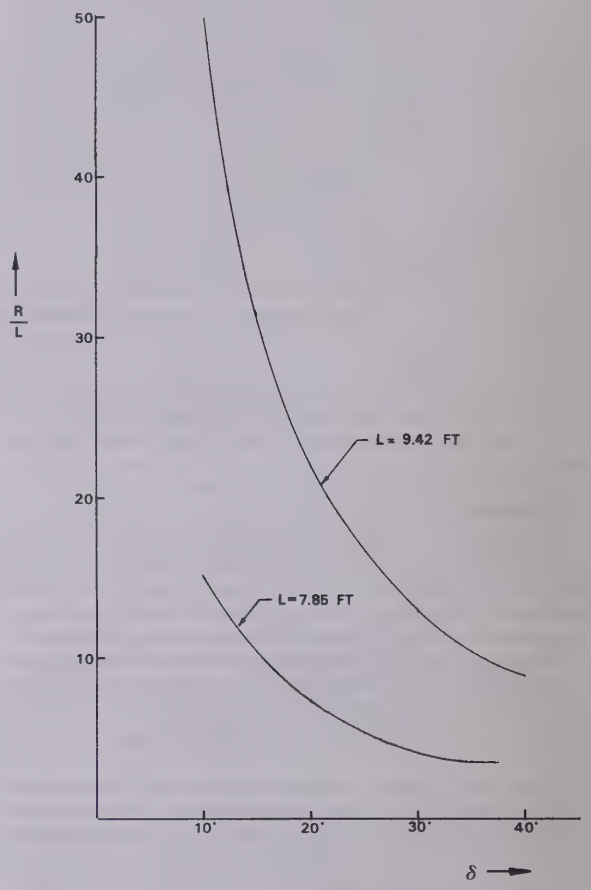

Fig. 23 Turning radius of length variation models

the owners' requirements and which produces the least-cost ship. This technique was first applied to ship design optimization by Mandel and Leopold [17]. The important calculations which the program carries out are listed in Table 17.

The most influential constraint in the program is the minimum acceptable level ice thickness which the owners desire the ship to negotiate at a constant speed (usually assumed to be 3 knots). Equation (2), which was derived from the extensive parametric tests described earlier, was formulated into a subroutine which permitted its solution for the value of level ice thickness which can be broken continuously, given the current values for ship breadth, draft, block coefficient, hull-ice friction factor, shaft horsepower, and desired speed of advance. With this subroutine incorporated into the program, it was run to check the major hull parameter selection of the preliminary design.

Running the Feasibility Design Model

Two runs of the model were made, one for the conditions provided by the designer (German and Milne) as summarized in Table 18, and one with a reduced level of endurance [16 full-power days (FPD)].

The main parameters of the two ships are

Endurance, FPD	21	16
Cost, $	181×10^6	155.8×10^6
LBP, ft	583.9	583.4
Beam, ft	100.54	91.83

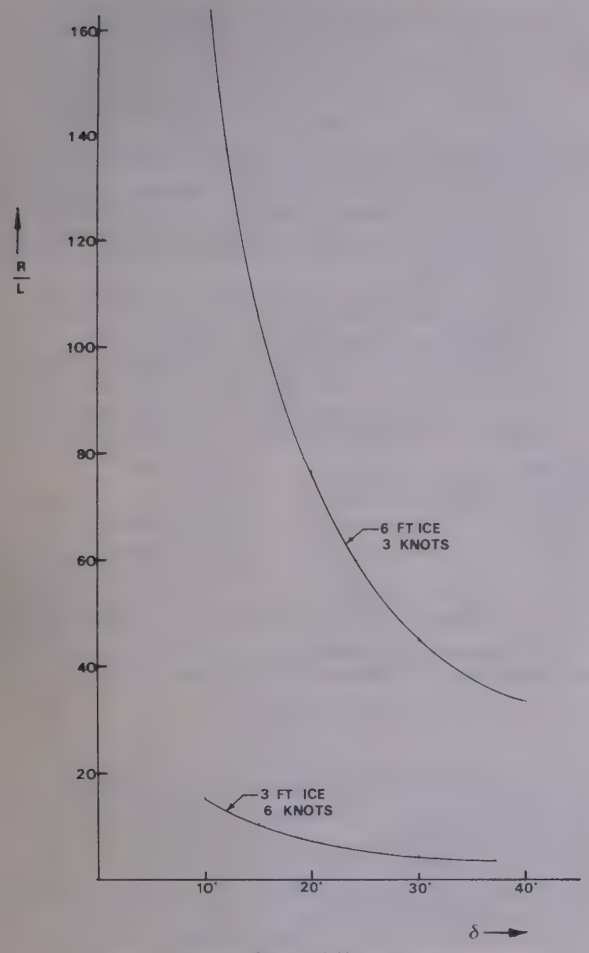

Fig. 24 Turning radius in differing ice thicknesses

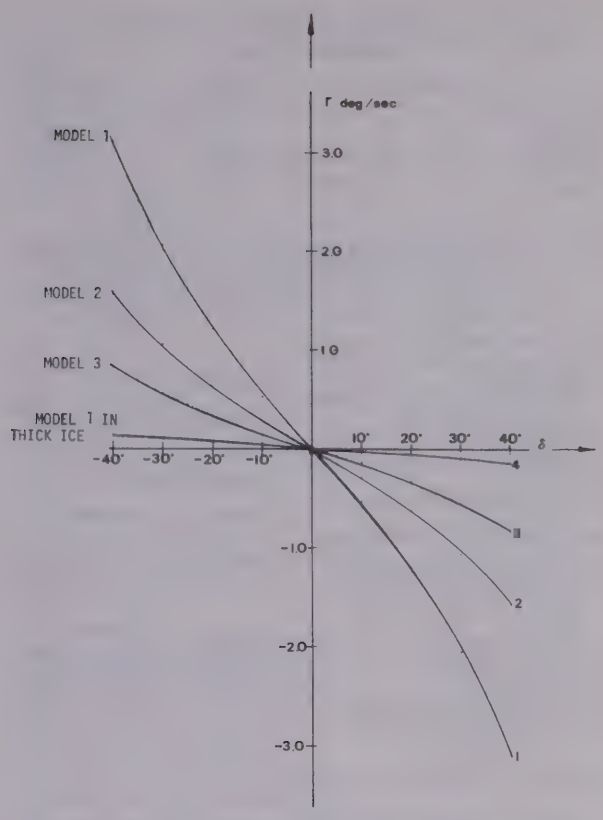

Fig. 25 Yaw velocity versus rudder angle for parametric models

Power, shp	83,866	83,089
Draft, ft	41.67	35.58
Full-load displacement, tons	37,119	29,977
Fuel weight, tons	9,362	7,053

Both ships are long, reflecting the fact that length does not influence resistance in the program, and increases the cost through the cubic number. The major cost in the program is the hull steel. It has been found, by regression analysis of icebreaker cost data, to be a linear function of cubic number. Consequently, an equal percent change in length, breadth, or depth produces an equal percent change in cost. Since decreasing breadth and draft reduces resistance, the length would not be reduced; rather, the beam and draft would be reduced. The beam, draft, and block coefficient seem to be interchangeably varied to achieve a minimum-cost ship.

The effect of endurance on ship size and cost for the same performance is significant. Changing endurance by 25 percent results in a 15 percent change in cost.

Summary and Conclusions

In this paper we described an extensive experimental program to support the rational selection of main hull parameters and installed power for a new Arctic icebreaker which would produce the lowest initial-cost ship consistent with the performance requirements of the Canadian Coast Guard. The program was divided into four elements, with certain objectives associated with each:

- *Model/full-scale correlation study and medium selection:*

(*a*) Assess the validity of model/full-scale correlation in ice fields ranging in thickness from 2 to 6 ft.

(*b*) Compare the capability of model ramming tests with that of towed tests for predicting full-scale continuous icebreaking performance.

(*c*) Assess the feasibility of using model tests in synthetic ice to predict full-scale continuous icebreaking performance in level ice.

(*d*) Assess the influence of friction and ice strength on the continuous icebreaking performance in level ice.

(*e*) Assess the influence of model scale on the predictive capability of towed model tests in saline ice.

- *Parametric ice resistance tests:*

Assess the influence of the variation of the hull parameters—beam, draft, length, and block coefficient—upon the continuous icebreaking performance of modern icebreaker-type hull in level ice.

- *Icebreaker maneuverability program:*

(*a*) Develop a technique for predicting the maneuvering characteristics of icebreaking ships while proceeding through level ice and compare the results obtained by this technique with full-scale results.

(*b*) Predict the effect of variations in length and block coefficient upon the turning capability of an icebreaker moving steadily through level ice.

Table 15 Directional stability criteria for parametric models

	Ice thickness, in.	Towing speed, fps	Stability criteria C'
Model 1	0.5	1.2	0.00161
Model 2	0.5	1.2	0.00334
Model 3	0.5	1.2	0.00382
Model 1	1.0	0.6	0.2947

Table 16 Owner's requirements which can be handled by the computerized Feasibility Design Program

ITEM	HOW ENTERED
Minimum desired continuous icebreaking resistance at a given speed	inequality constraint
Minimum endurance (expressed in full-power days)	inequality constraint
Minimum ramming-mode ice thickness (at a given impact speed)	inequality constraint
Minimum desirable free route speed	inequality constraint
Maximum or minimum beam, length, or draft	inequality constraint
Minimum acceptable *GM* in beached-on-ice condition (ramming speed—no ice failure)	inequality constraint
Accommodations	number input to program
Stores capacity	days input to program
Cargo capacity	weight input to program
Helicopter, oceanographic, communications, and control capacity	weight input

• *Least-cost hull selection program:*

Determine the major dimensions, required propulsive power, and cost of an Arctic icebreaker which meets the performance requirements stipulated by the owner.

Based upon the results of this program we conclude the following about each of the respective program elements:

• *Model/full-scale correlation study and media selection:*

(*a*) Satisfactory correlation between the performance of the CCGS *Louis S. St. Laurent* in level ice, as predicted by model tests in saline ice and measured during field tests, was obtained.

(*b*) Model tests to measure the resistance offered by level ice to the motion of a ship were conducted using constant-speed towing tests and nonpropelled, inertial ramming tests. Both predict similar values of resistance; however, the ramming tests exhibit large dispersion in the data. Hence, continuous towed tests are preferable.

(*c*) When the results of constant-speed towing tests in synthetic ice are used to predict full-scale performance, the full-scale results are on the high side. Due to logistic problems, such tests consume more time and labor than similar tests in saline ice. Furthermore, to control or vary hull-ice friction over several steps using synthetic ice requires the use of exotic coatings. Consequently, saline ice was considered to be the more flexible and cost-effective medium for subsequent tests.

(*d*) A variation in model ice flexural strength over the range of equivalent values of full-scale ice strength normally encountered in the Arctic (40 to 100 psi) produces a 40-percent change in mean speed of advance predicted for the CCGS *Louis S. St. Laurent* in level ice 3 ft thick at full power. A variation in model hull-ice friction factor from 0.1 to 0.4 produces a predicted 600 percent decrease in mean speed of advance under the same conditions. We conclude that the effect of strength on resistance is relatively small while that of friction factor is large.

(*e*) A scale effect is evident in model ice resistance tests. The $\frac{1}{48}$th-scale models predict higher resistance than the $\frac{1}{96}$th-scale models with divergence increasing from zero to 10 percent as ice thickness Froude number increases from zero to 2.0. At low speeds typical of the limiting conditions of icebreaker performance, scale effect is negligible.

• *Parametric resistance tests:*

Analysis of the results of the parametric resistance tests indicated the following for the range of variables tested:

1. Level ice resistance is a linear function of beam.
2. Level ice resistance is not significantly affected by changes in waterline length (although later tests showed length effect on maneuvering capability).
3. Level ice resistance increases linearly with increasing draft.
4. Level ice resistance increases nonlinearly with block coefficient.
5. The effect of draft and block coefficient on level ice resistance is large enough to influence the selection of parameters for an icebreaking ship with minimum initial cost in mind.

• *Icebreaker maneuverability program:*

(*a*) A technique was developed for predicting the steady-state turning circle and stability criteria for icebreaking ships operating in level ice. Model predictions for steady-state turning circle agree reasonably well with limited data available

Table 17 Important elements of Icebreaking Feasibility Design Program

1. Calculation of required freeboard.
2. Calculation of maximum ice thickness which can be broken in the ramming mode for a specified impact speed.
3. Calculation of available thrust (screw size limited by desired number, draft and breadth).
4. Thickness of level ice which can be broken in the continuous mode [a subroutine for solving equation (2) implicitely for ice thickness, given desired advance speed, beam, draft, block coefficient, available thrust, and ice strength).
5. Estimate of free route speed using actual model open-water resistance (dimensionless) for the M-13 hull (*Polar Star*).
6. Estimate of weights based upon regression analyses of weight data from *Wind*-Class, *Fuji, San Martin, Louis S. St. Laurent,* and *Glacier* as follows:

SYMBOL	U.S. NAVY WEIGHT GROUP	VARIABLE USED TO ESTIMATE
Hull steel	1	f (cubic No.)
Mach. & electrical	2 & 3	f (*SHP*)
Auxiliary systems	5	f (cubic No., *SHP* & complement)
Outfit	6	f (CN, comp, L_{BP}, D)
Loads	None	f (comp, days of stores)

7. Calculation of moments.
8. Calculation of *GM* at the conclusion of an unsuccessful ram.
9. Calculation of construction costs.
10. Calculation of allowable τ for 10 percent back cavitation.
11. Calculation of full-power days.

Table 18 Design conditions for *Polar VII*

Maximum beam, ft	106
Maximum draft, ft	42
Minimum endurance, full power days	21
Ramming-mode ice thickness, ft	25
Continuous-mode ice thickness	7 ft at 3.0 knots
Free running speed, knots	15

from two full-scale turning tests of the CCGS *Labrador*.

(*b*) Length, block coefficient, and ice thickness were identified as the variables strongly influencing steady-state turning circle in level ice.

• *Least-cost hull selection program:*

(*a*) The preliminary major dimensions of a least-cost Arctic ice-breaker were selected by an optimization program which incorporated the continuous ice resistance predictor equation derived from the parametric model tests. The results showed that the required endurance at full power has a strong influence on ship size and cost.

(*b*) It is particularly interesting to note that the final design parameters are in close agreement with the results of the Feasibility Design Program. The final selection of particulars was inevitably influenced by detailed considerations not included in the Feasibility Program, and differences between the two can therefore be expected. However, the agreement is nonetheless remarkably close, as the following tabulation shows:

Parameter	From Feasibility Program	Final Figures
Length, *BP*, ft	583.9	577.8
Draft, *LWL*, ft	41.7	40.6
Breadth, *LWL*, ft	100.5	101.6
Block coefficient	0.5117	0.535
Displacement, *LWL*, LT	35,772	36,405
Estimated cost, $ (1975)	182 M	165 M

Acknowledgments

The authors wish to thank the Canadian Coast Guard for permission to publish the results of the *Polar VII* Hull Development Program. It goes without saying that without the financial support of the Canadian Coast Guard, this program would never have been undertaken. It is, as far as we know, the first time that systematic tests of performance in ice have been intimately integrated into the design program for an icebreaker. Their foresight made it possible.

References

1 Melberg, L. C., Lewis, J. W., Edwards, R. Y., Jr., Taylor, R. G., and Voelker R. P., "The Design of Polar Icebreakers." SNAME Spring Meeting, 1970.

2 Kashtelyan, V. I., Poznjak, I. I., and Ryvlin, A. Ya., "Ice Resistance to Motion of a Ship," (translation), *Sudostroenie*, Leningrad, 1968.

3 Lewis, Jack W. and Edwards, R. Y., Jr., "Methods for Predicting Icebreaking and Ice Resistance Characteristics of Icebreakers," TRANS., SNAME Vol. 78, 1970.

4 Edwards, R. Y., Lewis, J. W., Wheaton, J. W., and Colburn, J., "Full Scale and Model Tests of a Great Lakes Icebreaker," TRANS. SNAME, Vol. 80, 1972.

5 Edwards, R. Y., Jr. and Lewis, J. W., "Modeling and Motions of Ships Through Polar Ice Fields Using Unconstrained Self-Propelled Models," IAHR Ice Symposium, Reykjanik, Iceland, 1970.

6 Kotras, T., Benze, D., and Blanten, B., "Length/Beam Effect on Icebreaking Resistance," SNAME Eastern Canadian Section, Fall meeting, 1974.

7 Enkvist, E., "On the Resistance Encountered by Ships Operating in the Continuous Mode of Icebreaking," Report No. 24, Swedish Academy of Engineering Sciences in Finland, 1972.

8 Johansson, B. M. and Makinen, Eero, "Icebreaking Model Tests: Systematic Variation of Bow Lines and Main Dimensions of Hull Forms Suitable for the Great Lakes," *Marine Technology*, Vol. 10, No. 3. July 1973.

9 Edwards R. Y., Jr., German, J. G., and Lawrence, R. G. A., "Comparative Model Tests of the Icebreaker Performance of Two Canadian Coast Guard Ice-breakers," Second International Conference on Port and Ocean Engineering Under Arctic Conditions, Reykavik, Iceland, Fall 1973.

10 Michel, B., "Ice Modeling in Hydraulic Engineering," International Association for Hydraulic Research Symposium—Ice Interaction on Hydraulic Structures, Sept. 7–10, 1970.

11 Crago, W. A., Dix, P. J., and German, J. G., "Model Icebreaking Experiments and Their Correlation with Hull Scale Data," *Trans.* RINA, Vol. 112, 1970.

12 Vance, G. P., "A Scaling System for Vessels in Ice," SNAME Ice Tech Symposium, Montreal, 1975.

13 German, J. G. and Lawrence, R. G. A., "Full Scale Testing in Ice of Three Icebreakers," SNAME Ice Tech Symposium, Montreal, 1975.

14 Abkowitz, M. A., "Lectures on Ship Hydrodynamics—Steering and Maneuverability," Report No. Hy-5 Hydro and Aerodynamics Laboratory, Lyngby, Denmark, May 1964.

15 *Principles of Naval Architecture*, John P. Comstock, Ed., (Revised ed.), SNAME, 1967.

16 *Principles of Naval Architecture*, H. E. Rossell and L. B. Chapman, Eds., Vol. 2, SNAME, 1962.

17 Mandel, P. and Leopold, R., "Optimization Methods Applied to Ship Design," TRANS. SNAME, Vol. 74, 1966, pp. 477–521.

(*Appendix Tables 19–36 follow*)

Appendix

Tabulated data

Table 19 Continuous-icebreaking resistance test results: 1/36th model test data—CCGS *Louis S. St. Laurent*

Date and Ice Sheet No.	Run No.	R (kg)	h (cm)	v (cm/sec)	σ_f (kg/cm²)	f —	E (kg/cm²)	E/σ_f —	$\frac{v}{\sqrt{gh}}$	$\frac{\sigma_f}{\rho_w gh}$	$\frac{R}{\rho_w gBh^2}$
1-27-75	1	2.88	3.99	2.30	0.21	0.08	119.00	567.	0.04	52.63	2.67
	2	4.97	3.97	19.49	0.21	0.08	119.00	567.	0.31	52.90	4.66
IS#1	3	5.01	3.82	37.88	0.17	0.08	119.00	700.	0.62	44.50	5.07
	4	5.76	3.81	55.43	0.17	0.08	119.00	700.	0.91	44.62	5.86
	5	6.61	3.84	73.10	0.17	0.08	119.00	700.	1.19	44.27	6.62
1-28-75	1	2.69	3.51	2.74	0.23	0.08	59.00	257.	0.05	65.53	3.23
	2	3.58	3.25	20.31	0.23	0.08	59.00	257.	0.36	70.77	5.01
IS#2	3	4.37	3.27	38.99	0.23	0.08	59.00	257.	0.69	70.34	6.04
	4	4.89	3.25	55.70	0.23	0.08	59.00	257.	0.99	70.77	6.84
	5	6.08	3.30	73.87	0.23	0.08	59.00	257.	1.30	69.70	8.25
1-29-75	1	1.34	2.35	2.46	0.21	0.08	96.00	457.	0.05	89.36	3.58
	2	2.03	2.40	20.64	0.21	0.08	96.00	457.	0.43	87.50	5.21
IS#3	3	3.05	2.47	39.25	0.21	0.08	96.00	457.	0.80	85.02	7.38
	4	3.41	2.48	57.05	0.14	0.08	96.00	686.	1.16	56.45	8.19
	5	4.27	2.44	74.66	0.14	0.08	96.00	686.	1.53	57.38	10.59
1-30-75	1	0.39	1.22	2.11	0.11	0.08	41.00	373.	0.06	90.16	3.87
	2	0.84	1.23	20.64	0.11	0.08	41.00	373.	0.59	89.43	8.20
IS#4	3	1.13	1.25	39.52	0.11	0.08	41.00	373.	1.13	88.00	10.68
	4	1.42	1.19	56.14	0.11	0.08	41.00	373.	1.64	92.44	14.81
	5	2.00	1.20	74.26	0.11	0.08	41.00	373.	2.16	91.67	20.52
1-31-75	1	2.73	3.50	3.24	0.21	0.10	81.00	386.	0.06	60.00	3.29
	2	4.43	3.47	20.70	0.21	0.10	81.00	386.	0.35	60.52	5.43
IS#5	3	5.01	3.50	40.33	0.21	0.10	81.00	386.	0.69	60.00	6.04
	4	5.48	3.64	55.70	0.21	0.10	81.00	386.	0.93	57.69	6.11
	5	6.93	3.73	77.88	0.21	0.10	81.00	386.	1.29	56.30	7.36
2-4-75	1	1.75	1.90	2.80	0.35	0.29	46.00	131.	0.06	184.21	7.16
	2	2.94	2.04	26.44	0.35	0.29	46.00	131.	0.59	171.57	10.44
IS#6	3	3.31	1.88	40.00	0.35	0.29	46.00	131.	0.93	186.17	13.83
	4	4.20	1.87	56.39	0.35	0.29	46.00	131.	1.32	187.17	17.74
	5	5.40	1.90	71.76	0.35	0.29	46.00	131.	1.66	184.21	22.10
2-5-75	1	0.77	1.08	3.30	0.21	0.29	68.00	324.	0.10	194.44	9.75
	2	1.24	1.08	21.08	0.21	0.29	68.00	324.	0.65	194.44	15.70
IS#7	3	1.42	1.00	39.66	0.21	0.29	68.00	324.	1.27	210.00	20.97
	4	1.96	1.06	57.92	0.21	0.29	68.00	324.	1.80	198.11	25.77
	5	2.43	1.10	76.97	0.21	0.29	68.00	324.	2.34	190.91	29.66
2-7-75	1	2.99	2.92	2.88	0.21	0.29	18.00	86.	0.05	71.92	5.18
	2	3.95	2.93	22.08	0.21	0.29	18.00	86.	0.41	71.67	6.80
IS#8	3	5.12	3.04	41.05	0.21	0.29	18.00	86.	0.75	69.08	8.18
	4	6.18	3.13	57.92	0.21	0.29	18.00	86.	1.05	67.09	9.32
	5	8.75	3.35	76.97	0.21	0.29	18.00	86.	1.34	62.69	11.52
2-11-75	1	4.07	3.30	3.03	0.25	0.29	20.00	80.	0.05	75.76	5.52
	2	4.80	3.30	21.27	0.25	0.29	20.00	80.	0.37	75.76	6.51
IS#9	3	6.48	3.40	39.66	0.25	0.29	20.00	80.	0.69	73.53	8.28
	4	9.09	3.39	57.35	0.25	0.29	20.00	80.	0.99	73.75	11.68
	5	10.71	3.53	75.48	0.25	0.29	20.00	80.	1.28	70.82	12.70
2-12-75	1	1.28	2.25	2.83	0.25	0.12	19.00	76.	0.06	111.11	3.73
	2	2.77	2.59	20.89	0.25	0.12	19.00	76.	0.41	96.53	6.10
IS#10	3	3.52	2.65	39.66	0.25	0.12	19.00	76.	0.78	94.34	7.40
	4	4.16	2.70	57.92	0.25	0.12	19.00	76.	1.13	92.59	8.43
	5	4.69	2.61	75.97	0.25	0.12	19.00	76.	1.50	95.79	10.17
2-12-75	1	0.54	1.35	3.15	0.22	0.12	Elastic Modulus		0.09	162.96	4.38
	2	1.15	1.40	21.27	0.22	0.12	was not measured		0.57	157.14	8.67
IS#11	3	1.55	1.42	39.00	0.22	0.12	↓	↓	1.05	154.93	11.35
	4	1.90	1.43	57.07	0.22	0.12			1.52	153.85	13.72
	5	2.51	1.44	73.12	0.22	0.12	↓	↓	1.95	152.78	17.88
2-13-75	1	3.03	3.15	2.89	0.25	0.12	23.00	92.	0.05	79.37	4.51
	2	4.05	3.28	20.89	0.25	0.12	23.00	92.	0.37	76.22	5.56
IS#12	3	4.69	3.39	39.66	0.25	0.12	23.00	92.	0.69	73.75	6.03
	4	4.91	3.40	57.07	0.25	0.12	23.00	92.	0.99	73.53	6.27
	5	6.19	3.45	75.00	0.25	0.12	23.00	92.	1.29	72.46	7.68
2-14-75	1	1.56	2.86	2.97	0.21	0.12	13.00	62.	0.06	73.43	2.82
	2	3.05	3.15	20.17	0.21	0.12	13.00	62.	0.36	66.67	4.54
IS#13	3	3.52	3.05	39.66	0.21	0.12	13.00	62.	0.73	68.85	5.59
	4	3.52	2.75	57.35	0.17	0.12	13.00	76.	1.10	61.82	6.88
	5	4.09	2.63	75.00	0.17	0.12	13.00	76.	1.48	64.64	8.73
2-18-75	1	2.35	1.88	2.60	0.22	0.48	9.00	41.	0.06	117.02	9.82
	2	5.87	1.94	39.66	0.22	0.48	9.00	41.	0.91	113.40	23.04
IS#14	3	11.73	2.22	75.97	0.22	0.48	9.00	41.	1.63	99.10	35.16
	4	1.54	2.34	2.80	0.02	0.48	9.00	450.	0.06	8.55	4.15
	5	4.73	2.16	35.46	0.02	0.48	9.00	450.	0.77	9.26	14.97
	6	5.76	2.10	74.05	0.02	0.48	9.00	450.	1.63	9.52	19.29
2-19-75	1	4.20	2.60	2.98	0.14	0.48	79.00	564.	0.06	53.85	9.18
	2	9.85	3.05	39.00	0.14	0.48	79.00	564.	0.71	45.90	15.64
IS#15	3	13.14	3.10	75.00	0.14	0.48	79.00	564.	1.36	45.16	20.20
	4	3.28	2.90	2.90	0.02	0.48	79.00	3950.	0.05	6.90	5.76
	5	9.30	2.50	39.30	0.02	0.48	79.00	3950.	0.79	8.00	21.98
	6	8.62	2.45	75.50	0.02	0.48	79.00	3950.	1.54	8.16	21.21
2-19-75	1	1.44	1.23	2.70	0.21	0.48			0.08	170.73	14.06
	2	2.78	1.19	39.00	0.21	0.48	Elastic Modulus		1.14	176.47	29.00
IS#16	3	6.19	1.29	76.00	0.21	0.48	was not measured		2.14	168.79	54.94
	4	1.57	1.18	2.73	0.09	0.48			0.08	76.27	16.66
	5	2.95	1.20	39.80	0.09	0.48	↓	↓	1.16	75.00	30.26
	6	3.95	1.08	76.00	0.09	0.48			2.34	83.33	50.02

Table 20 Continuous-icebreaking resistance test results: 1/48th model test data—CCGS *Louis S. St. Laurent*

Date and Ice Sheet No.	Run No.	R (kg)	h (cm)	v (cm/sec)	σ_f (kg/cm²)	f —	E (kg/cm²)	E/σ_f	$\frac{v}{\sqrt{gh}}$	$\frac{\sigma_f}{\rho_w g h}$	$\frac{R}{\rho_w g b h^2}$
1-27-75	1	2.44	4.00	2.30	0.21	0.12	119.00	567.	0.04	52.50	3.00
IS#1	2	3.67	3.95	19.49	0.21	0.12	119.00	567.	0.31	53.16	4.48
	3	4.64	3.95	37.88	0.17	0.12	119.00	700.	0.61	43.04	5.84
	4	5.10	3.88	55.43	0.17	0.12	119.00	700.	0.90	43.81	6.66
	5	5.91	3.86	73.10	0.17	0.12	119.00	700.	1.19	44.04	7.79
1-28-75	1	2.39	3.58	2.74	0.23	0.12	59.00	257.	0.05	64.07	3.64
IS#2	2	3.27	3.50	20.31	0.23	0.12	59.00	257.	0.35	65.71	5.24
	3	3.77	3.44	38.99	0.23	0.12	59.00	257.	0.67	66.86	6.26
	4	3.77	3.21	55.70	0.23	0.12	59.00	257.	0.99	71.65	7.19
	5	4.37	3.27	73.87	0.23	0.12	59.00	257.	1.30	70.34	7.85
1-29-75	1	1.08	2.35	2.46	0.21	0.12	96.00	457.	0.05	89.36	3.84
IS#3	2	2.01	2.40	20.64	0.21	0.12	96.00	457.	0.43	87.50	6.86
	3	2.79	2.50	39.25	0.21	0.12	96.00	457.	0.79	84.00	8.77
	4	3.02	2.50	57.05	0.14	0.12	96.00	686.	1.15	56.00	9.49
	5	3.77	2.45	74.66	0.14	0.12	96.00	686.	1.52	57.14	12.34
1-30-75	1	0.36	1.27	2.11	0.11	0.12	41.00	373.	0.06	86.61	4.39
IS#4	2	0.70	1.27	20.64	0.11	0.12	41.00	373.	0.58	86.61	8.53
	3	0.98	1.28	39.52	0.11	0.12	41.00	373.	1.12	85.94	11.75
	4	1.24	1.23	56.14	0.11	0.12	41.00	373.	1.62	89.43	16.10
	5	1.61	1.29	74.26	0.11	0.12	41.00	373.	2.09	85.27	19.01
1-31-75	1	2.34	3.50	3.24	0.21	0.16	81.00	386.	0.06	60.00	3.75
IS#5	2	4.27	3.47	20.70	0.21	0.16	81.00	386.	0.35	60.52	6.97
	3	4.80	3.53	40.33	0.21	0.16	81.00	386.	0.69	59.49	7.57
	4	5.15	3.54	55.70	0.21	0.16	81.00	386.	0.95	59.32	8.07
	5	5.91	3.61	77.88	0.21	0.16	81.00	386.	1.31	58.17	8.91
2-4-75	1	1.26	1.92	2.80	0.35	0.28	46.00	131.	0.06	182.29	6.72
IS#6	2	2.31	2.00	26.44	0.35	0.28	46.00	131.	0.60	175.00	11.35
	3	2.64	1.90	40.00	0.35	0.28	46.00	131.	0.93	184.21	14.37
	4	2.99	1.82	56.39	0.35	0.28	46.00	131.	1.33	192.31	17.73
	5	4.27	1.88	71.76	0.35	0.28	46.00	131.	1.67	186.17	20.74
2-5-75	1	0.77	1.15	3.30	0.21	0.28	68.00	324.	0.10	182.61	11.44
IS#7	2	1.09	1.12	21.08	0.21	0.28	68.00	324.	0.64	187.50	17.07
	3	1.46	1.05	39.66	0.21	0.28	68.00	324.	1.24	200.00	26.02
	4	1.71	1.06	57.92	0.21	0.28	68.00	324.	1.80	198.11	29.90
	5	2.56	1.15	76.97	0.21	0.28	68.00	324.	2.29	182.61	38.03
2-7-75	1	2.34	2.94	2.88	0.21	0.28	18.00	86.	0.05	71.43	5.32
IS#8	2	3.14	2.85	22.08	0.21	0.28	18.00	86.	0.42	73.68	7.59
	3	4.15	2.98	41.05	0.21	0.28	18.00	86.	0.76	70.47	9.18
	4	5.65	3.18	57.92	0.21	0.28	18.00	86.	1.04	66.04	10.98
	5	7.61	3.38	76.97	0.21	0.28	18.00	86.	1.34	62.13	13.09
2-11-75	1	3.57	3.30	3.03	0.25	0.38	20.00	80.	0.05	75.76	6.44
IS#9	2	5.28	3.48	21.27	0.25	0.28	20.00	80.	0.36	71.84	8.57
	3	6.79	3.40	39.66	0.25	0.28	20.00	80.	0.69	73.53	11.54
	4	7.92	3.45	57.35	0.25	0.28	20.00	80.	0.99	72.46	13.07
	5	9.67	3.60	75.48	0.25	0.28	20.00	80.	1.27	69.44	14.66
2-12-75	1	1.00	2.16	2.83	0.25	0.19	19.00	76.	0.06	115.74	4.31
IS#10	2	1.86	2.37	20.89	0.25	0.19	19.00	76.	0.43	105.49	6.51
	3	3.02	2.53	39.66	0.25	0.19	19.00	76.	0.80	98.81	9.37
	4	3.14	2.58	57.92	0.25	0.19	19.00	76.	1.15	96.90	9.27
	5	3.84	2.62	75.97	0.25	0.19	19.00	76.	1.50	95.42	10.39
2-12-75	1	0.60	1.34	3.15	0.22	0.19	Elastic Modulus		0.09	164.18	6.56
IS#11	2	0.95	1.38	21.27	0.22	0.19	was not measured		0.58	159.42	9.80
	3	1.36	1.42	39.00	0.22	0.19	↓	↓	1.05	154.93	13.25
	4	1.59	1.40	57.07	0.22	0.19			1.54	157.14	15.94
	5	2.12	1.43	73.12	0.22	0.19			1.95	153.85	20.37
2-13-75	1	2.41	3.17	2.89	0.25	0.19	23.00	92.	0.05	78.86	4.71
IS#12	2	3.27	3.30	20.89	0.25	0.19	23.00	92.	0.37	75.76	5.90
	3	4.02	3.38	39.66	0.25	0.19	23.00	92.	0.69	73.96	6.91
	4	4.52	3.45	57.07	0.25	0.19	23.00	92.	0.98	72.46	7.46
	5	5.03	3.50	75.00	0.25	0.19	23.00	92.	1.28	71.43	8.07
2-14-75	1	1.21	2.65	2.97	0.21	0.19	13.00	62.	0.06	79.68	3.93
IS#13	2	2.29	3.10	20.17	0.21	0.19	13.00	62.	0.37	67.74	4.68
	3	3.02	3.05	39.66	0.21	0.19	13.00	62.	0.73	68.85	6.38
	4	3.14	2.75	57.35	0.17	0.19	13.00	76.	1.10	61.82	8.16
	5	3.52	2.67	75.00	0.17	0.19	13.00	76.	1.47	63.67	9.70
2-18-75	1	2.06	1.87	2.60	0.22	0.40	9.00	41.	0.06	117.65	11.57
IS#14	2	4.65	2.09	39.66	0.22	0.40	9.00	41.	0.88	105.26	20.91
	3	6.66	2.23	75.97	0.22	0.40	9.00	41.	1.62	98.65	28.31
	4	1.21	2.39	2.80	0.02	0.40	9.00	450.	0.06	8.37	4.16
	5	3.78	2.22	35.46	0.02	0.40	9.00	450.	0.76	9.01	15.07
	B	4.15	2.03	74.05	0.02	0.40	9.00	450.	1.84	9.62	18.85
2-19-75	1	2.03	2.57	2.98	0.14	0.40	79.00	564.	0.06	54.47	6.04
IS#15	2	6.71	2.98	39.00	0.14	0.40	79.00	564.	0.72	46.98	14.84
	3	9.05	3.25	75.00	0.14	0.40	79.00	564.	1.33	43.08	16.88
	4	1.91	3.05	2.90	0.02	0.40	79.00	3950.	0.05	6.56	4.03
	5	5.78	2.73	39.30	0.02	0.40	79.00	3950.	0.76	7.33	15.24
	6	6.18	2.48	75.50	0.02	0.40	79.00	3950.	1.53	8.06	19.74
2-19-75	1	1.14	1.17	2.70	0.21	0.40	Elastic Modulus		0.08	179.49	16.36
IS#16	2	2.06	1.22	39.00	0.21	0.40	was not measured		1.13	172.13	27.19
	3	4.02	1.30	76.00	0.21	0.40			2.13	161.54	46.73
	4	1.17	1.23	2.73	0.09	0.40			0.08	73.17	15.19
	5	1.91	1.16	39.80	0.09	0.40			1.18	77.59	27.89
	6	3.39	1.06	76.00	0.09	0.40	↓	↓	2.36	84.91	59.27

Table 21 1/36th model ramming test results—CCGS *Louis S. St. Laurent*

Date and Ice Sheet No.	Charge No.	R (kg)	h (cm)	v (cm/sec)	σ_f (kg/cm²)	$\frac{v}{\sqrt{gh}}$	$\frac{\sigma_f}{\rho_w ph}$	$\frac{R}{\rho_w gBh^2}$
2-24-75	1	10.11	3.80	69.00	0.19	1.130	50.00	10.34
IS#1		9.03	3.80	46.00	0.19	0.754	50.00	9.24
		7.77	3.80	23.00	0.19	0.377	50.00	7.95
		5.87	3.80	11.00	0.19	0.180	50.00	6.00
		4.74	3.80	5.50	0.19	0.090	50.00	4.85
"	2	10.92	3.80	115.00	0.19	1.884	50.00	11.17
		9.34	3.80	92.00	0.19	1.507	50.00	9.55
		8.38	3.80	69.00	0.19	1.130	50.00	8.57
		7.51	3.80	46.00	0.19	0.754	50.00	7.68
		7.01	3.80	23.00	0.19	0.377	50.00	7.17
		6.57	3.80	11.00	0.19	0.180	50.00	6.72
		4.61	3.80	5.50	0.19	0.090	50.00	4.72
"	3	9.72	3.85	69.00	0.19	1.123	49.35	9.69
		9.34	3.85	46.00	0.19	0.749	49.35	9.31
		8.71	3.85	23.00	0.19	0.374	49.35	8.68
		7.51	3.85	11.00	0.19	0.179	49.35	7.48
		5.49	3.85	5.50	0.19	0.090	49.35	5.47
"	4	12.94	4.08	115.00	0.19	1.818	46.57	11.48
		11.87	4.08	92.00	0.19	1.454	46.57	10.53
		9.72	4.08	69.00	0.19	1.091	46.57	8.62
		8.40	4.08	46.00	0.19	0.727	46.57	7.45
		8.08	4.08	23.00	0.19	0.364	46.57	7.17
		7.51	4.08	11.50	0.19	0.182	46.57	6.66
"	5	10.60	3.85	115.00	0.19	1.872	49.35	10.56
		8.84	3.85	92.00	0.19	1.497	49.35	8.81
		7.58	3.85	69.00	0.19	1.123	49.35	7.55
		6.44	3.85	46.00	0.19	0.749	49.35	6.42
		5.37	3.85	23.00	0.19	0.374	49.35	5.35
		3.41	3.85	11.50	0.19	0.187	49.35	3.40
	6	2.65	3.85	5.70	0.19	0.093	49.35	2.64
2-25-75		8.21	3.53	69.00	0.19	1.173	53.82	9.73
IS#1		6.44	3.53	46.00	0.19	0.782	53.82	7.63
		5.62	3.53	23.00	0.19	0.391	53.82	6.66
		4.61	3.53	11.50	0.19	0.195	53.82	5.46
2-25-75	1	4.10	2.58	93.00	0.08	1.849	31.01	9.10
IS#2		3.62	2.58	69.00	0.08	1.372	31.01	8.03
		3.14	2.58	46.00	0.08	0.915	31.01	6.97
		2.69	2.58	23.00	0.08	0.457	31.01	5.97
	2	7.89	2.72	140.00	0.08	2.711	29.41	15.75
		6.16	2.72	115.00	0.08	2.227	29.41	12.30
"		5.10	2.72	93.00	0.08	1.801	29.41	10.18
		5.10	2.72	69.00	0.08	1.336	29.41	10.18
		4.60	2.72	46.00	0.08	0.891	29.41	9.18
		3.86	2.72	23.00	0.08	0.445	29.41	7.71
	3	8.19	2.80	140.00	0.08	2.672	28.57	15.43
		7.26	2.80	115.00	0.08	2.195	28.57	13.68
		6.16	2.80	93.00	0.08	1.775	28.57	11.61
"		5.08	2.80	69.00	0.08	1.317	28.57	9.57
		4.60	2.80	46.00	0.08	0.878	28.57	8.67
		3.62	2.80	23.00	0.08	0.439	28.57	6.82
	4	4.60	2.75	93.00	0.08	1.791	29.09	8.98
		3.86	2.75	69.00	0.08	1.329	29.09	7.54
"		3.14	2.75	46.00	0.08	0.886	29.09	6.13
		2.69	2.75	23.00	0.08	0.443	29.09	5.25
	5	3.63	2.52	69.00	0.08	1.388	31.75	8.44
		2.79	2.52	46.00	0.08	0.925	31.75	6.49
		2.57	2.52	23.00	0.08	0.463	31.75	5.98
		2.57	2.52	11.00	0.08	0.221	31.75	5.98
		2.11	2.52	5.50	0.08	0.111	31.75	4.91
2-25-75	1	11.78	4.05	92.00	0.35	1.460	86.42	10.61
IS# 3		11.57	4.05	69.00	0.35	1.095	86.42	10.42
		10.78	4.05	46.00	0.35	0.730	86.42	9.71
		9.18	4.05	23.00	0.35	0.365	86.42	8.27
		5.62	4.05	11.00	0.35	0.175	86.42	5.06
		3.38	4.05	5.50	0.35	0.087	86.42	3.04
"	2	15.05	4.40	115.00	0.35	1.751	79.55	11.48
		14.79	4.40	92.00	0.35	1.401	79.55	11.28
		14.79	4.40	69.00	0.35	1.050	79.55	11.28
		13.08	4.40	46.00	0.35	0.700	79.55	9.98
		11.37	4.40	23.00	0.35	0.350	79.55	8.67
		9.18	4.40	11.00	0.35	0.167	79.55	7.00
		7.00	4.40	5.50	0.35	0.084	79.55	5.34
"	3	16.17	4.70	115.00	0.35	1.694	74.47	10.81
		14.53	4.70	92.00	0.35	1.355	74.47	9.72
		13.78	4.70	69.00	0.35	1.016	74.47	9.21
		13.78	4.70	46.00	0.35	0.678	74.47	9.21
		12.13	4.70	23.00	0.35	0.339	74.47	8.11
		9.18	4.70	11.00	0.35	0.162	74.47	6.14
		7.29	4.70	5.50	0.35	0.081	74.47	4.87
"	4	14.53	4.95	115.00	0.15	1.651	30.30	8.76
		12.63	4.95	92.00	0.15	1.321	30.30	7.61
		9.34	4.95	68.00	0.15	0.976	30.30	5.63
		7.74	4.95	46.00	0.15	0.660	30.30	4.67
		6.86	4.95	23.00	0.15	0.330	30.30	4.14
		6.43	4.95	11.00	0.15	0.158	30.30	3.88
		5.49	4.95	5.50	0.15	0.079	30.30	3.31

(*Cont'd*)

Table 21 (*Continued*)

Date and Ice Sheet No.	Charge No.	R (kg)	h (cm)	v (cm/sec)	σ_f (kg/cm²)	$\frac{v}{\sqrt{gh}}$	$\frac{\sigma_f}{\rho_w gh}$	$\frac{R}{\rho_w g b h^2}$
2-25-65	5	11.78	4.95	115.00	0.15	1.651	30.30	7.10
		10.79	4.95	92.00	0.15	1.321	30.30	6.50
IS#3		10.23	4.95	69.00	0.15	0.990	30.30	6.17
		10.04	4.95	46.00	0.15	0.660	30.30	6.05
		8.36	4.95	23.00	0.15	0.330	30.30	5.04
		7.15	4.95	11.00	0.15	0.158	30.30	4.31
		5.76	4.95	5.50	0.15	0.079	30.30	3.47
"	6	10.98	4.98	69.00	0.15	0.987	30.12	6.54
		9.51	4.98	46.00	0.15	0.658	30.12	5.66
		8.20	4.98	23.00	0.15	0.329	30.12	4.88
		6.72	4.98	11.00	0.15	0.157	30.12	4.00
		5.10	4.98	5.50	0.15	0.079	30.12	3.04
"	7	13.08	4.98	92.00	0.15	1.317	30.12	7.79
		10.79	4.98	69.00	0.15	0.987	30.12	6.43
		10.05	4.98	46.00	0.15	0.658	30.12	5.99
		10.05	4.98	23.00	0.15	0.329	30.12	5.99
		9.52	4.98	11.00	0.15	0.157	30.12	5.67
		7.15	4.98	5.50	0.15	0.079	30.12	4.26

Table 22 1/48th model ramming test results—CCGS *Louis S. St. Laurent*

Date and Ice Sheet No.	Charge No.	R (kg)	h (cm)	v (cm/sec)	σ_f (kg/cm²)	$\frac{v}{\sqrt{gh}}$	$\frac{\sigma_f}{\rho_w gh}$	$\frac{R}{\rho_w g B h^2}$
2-24-75	1	9.18	3.75	115.00	0.19	1.896	50.67	12.83
		7.63	3.75	93.00	0.19	1.534	50.67	10.66
IS #1		6.69	3.75	69.00	0.19	1.138	50.67	9.35
		6.36	3.75	46.00	0.19	0.759	50.67	8.89
		5.53	3.75	23.00	0.19	0.379	50.67	7.73
"	2	8.07	3.78	115.00	0.19	1.889	50.26	11.10
		7.08	3.78	93.00	0.19	1.528	50.26	9.73
		6.61	3.78	69.00	0.19	1.133	50.26	9.09
		5.92	3.78	46.00	0.19	0.756	50.26	8.14
		4.98	3.78	23.00	0.19	0.378	50.26	6.85
"	3	8.85	3.84	115.00	0.19	1.874	49.48	11.79
		7.08	3.84	93.00	0.19	1.516	49.48	9.43
		6.58	3.84	69.00	0.19	1.124	49.48	8.77
		6.14	3.84	46.00	0.19	0.750	49.48	8.18
		5.53	3.84	23.00	0.19	0.375	49.48	7.37
"	4	9.57	4.00	140.00	0.19	2.235	47.50	11.75
		7.91	4.00	115.00	0.19	1.836	47.50	9.71
		7.08	4.00	93.00	0.19	1.485	47.50	8.69
		6.14	4.00	69.00	0.19	1.102	47.50	7.54
		5.53	4.00	46.00	0.19	0.734	47.50	6.79
		4.98	4.00	23.00	0.19	0.367	47.50	6.11
"	5	8.52	3.95	115.00	0.19	1.848	48.10	10.73
		7.08	3.95	93.00	0.19	1.494	48.10	8.92
		6.58	3.95	69.00	0.19	1.109	48.10	8.29
		6.14	3.95	46.00	0.19	0.739	48.10	7.73
		5.37	3.95	23.00	0.19	0.370	48.10	6.76
"	6	7.91	3.65	115.00	0.19	1.922	52.05	11.66
		6.36	3.65	93.00	0.19	1.554	52.05	9.38
		5.92	3.65	69.00	0.19	1.153	52.05	8.73
		4.64	3.65	46.00	0.19	0.769	52.05	6.84
		4.31	3.65	23.00	0.19	0.384	52.05	6.36
2-24-75	7	8.51	3.31	115.00	0.19	2.019	57.40	15.26
		7.38	3.31	93.00	0.19	1.632	57.40	13.13
IS #1		6.36	3.31	69.00	0.19	1.211	57.40	11.40
		5.34	3.31	46.00	0.19	0.807	57.40	9.58
		4.77	3.31	23.00	0.19	0.404	57.40	8.55
2-25-75	1	4.81	2.51	115.00	0.17	2.318	67.73	15.00
		4.24	2.51	92.00	0.17	1.854	67.73	13.22
IS #2		3.73	2.51	69.00	0.17	1.391	67.73	11.63
		3.26	2.51	46.00	0.17	0.927	67.73	10.17
		2.70	2.51	23.00	0.17	0.464	67.73	9.36
		2.38	2.51	11.00	0.17	0.222	67.73	8.98
		1.80	2.51	5.50	0.17	0.111	67.73	5.61
"	2	5.16	2.85	115.00	0.17	2.175	59.65	12.48
		4.35	2.85	92.00	0.17	1.740	59.65	10.28
		3.73	2.85	69.00	0.17	1.305	59.65	9.02
		3.66	2.85	46.00	0.17	0.870	59.65	8.85
		3.25	2.85	23.00	0.17	0.435	59.65	7.86
		2.52	2.85	11.00	0.17	0.208	59.65	6.10
		1.74	2.85	5.50	0.17	0.104	59.65	4.21
"	3	4.72	2.87	92.00	0.17	1.734	59.23	11.26
		3.73	2.87	69.00	0.17	1.301	59.23	8.90
		3.39	2.87	46.00	0.17	0.867	59.23	8.09
		2.88	2.87	23.00	0.17	0.434	59.23	6.87
		2.23	2.87	11.00	0.17	0.207	59.23	5.32
		1.79	2.87	5.50	0.17	0.104	59.23	4.27

(*Cont'd*)

Table 22 (*Continued*)

Date and Ice Sheet No.	Charge No.	R (kg)	h (cm)	v (cm/sec)	σ_f (kg/cm²)	$\frac{v}{\sqrt{gh}}$	$\frac{\sigma_f}{\rho_w g h}$	$\frac{R}{\rho_w g B h^2}$
2-25-75	4	5.24	2.60	115.00	0.17	2.278	65.38	15.23
		4.97	2.60	92.00	0.17	1.822	65.38	14.44
IS#2		4.47	2.60	69.00	0.17	1.367	65.38	12.99
		3.80	2.60	46.00	0.17	0.911	65.38	11.04
		2.58	2.60	23.00	0.17	0.456	65.38	7.50
		1.89	2.60	11.00	0.17	0.218	65.38	5.49
"	5	1.53	2.60	5.50	0.17	0.109	65.38	4.45
		4.16	2.55	115.00	0.17	2.300	66.67	12.57
		3.45	2.55	92.00	0.17	1.840	66.67	10.42
		3.19	2.55	69.00	0.17	1.380	66.67	9.64
		2.58	2.55	46.00	0.17	0.920	66.67	7.80
		2.40	2.55	23.00	0.17	0.460	66.67	7.25
		2.23	2.55	11.00	0.17	0.220	66.67	6.74
		1.79	2.55	5.50	0.17	0.110	66.67	5.41

Table 23 Continuous-icebreaking resistance tests: 1/48th model test data in synthetic ice—CCGS *Louis S. St. Laurent*

Ice Sheet Number	Run Number	R (kg)	h (cm)	v (cm/sec)	σ_f (kg/cm²)	E (kg/cm²)	E/σ_f	σ_c (kg/cm²)	Friction
1	1	1.8	1.91	5.8	.18	96	533	.40	-
1	2	6.3	1.65	90.0	.18	96	533	.40	-
1	3	3.3	1.25	43.2	.18	96	533	.40	-
2	1	1.3	1.02	12.3	.17	-	-	.20	.56
2	2	6.3	1.03	93.6	.17	-	-	.20	.56
2	3	3.4	1.02	46.5	.17	-	-	.20	.56
3	1	5.4	2.90	7.0	.30	220	666	.23	.51
3	2	18.8	3.00	84.7	.30	220	666	.23	.51
3	3	9.6	3.00	41.0	.30	220	666	.23	.51
4	1	4.6	2.50	6.2	.26	173	665	.20	-
4	2	12.2	2.50	82.9	.26	173	665	.28	-
4	3	6.8	2.50	38.7	.26	173	665	.28	-
5	1	3.5	1.79	7.2	.87	875	1006	1.18	-
5	2	7.9	1.87	85.2	.87	875	1006	1.18	-
5	3	6.4	1.94	39.7	.87	875	1006	1.18	-
6	1	1.9	1.12	3.7	1.32	1639	1241	.92	.44
6	2	5.0	.97	82.3	1.32	1639	1241	.92	.44
6	3	2.6	.90	39.9	1.32	1639	1241	.92	.44
7	1	5.4	2.53	7.0	.97	933	961	.97	.50
7	2	12.9	2.49	81.0	.97	933	961	.97	.50
7	3	9.8	2.48	41.1	.97	933	961	.97	.50
8	1	6.2	2.73	6.5	.87	574	659	1.32	.18
8	2	12.9	2.78	66.8	.87	574	659	1.32	.18
8	3	11.2	2.74	41.1	.87	574	659	1.32	.18
8	4	9.8	2.74	25.1	.87	574	659	1.32	.18
* 9	1	.9	1.66	5.8	.63	3327	5280	.97	.14
* 9	2	2.1	1.43	60.2	.63	3327	5280	.97	.14
* 9	3	1.4	1.32	36.6	.63	3327	5280	.97	.14
10	1	1.9	2.03	6.2	.51	1946	3815	.58	.15
10	2	6.0	2.08	69.4	.51	1946	3815	.58	.15
10	3	4.3	2.14	38.6	.51	1946	3815	.58	.15
10	4	3.0	2.15	27.0	.51	1946	3815	.58	.15
11	1	2.6	2.25	3.5	.51	1227	2406	.59	.12
11	2	5.2	2.23	81.1	.51	1227	2406	.59	.12
11	3	3.3	2.53	24.4	.51	1227	2406	.59	.12
11	4	3.7	2.51	41.9	.51	1227	2406	.59	.12

* Many cracks in the ice sheet

Table 23 (*Continued*)

Ice Sheet Number	Run Number	R (kg)	h (cm)	v (cm/sec)	σ_f (kg/cm²)	E (kg/cm²)	E/σ_f	σ_c (kg/cm²)	Friction
12	1	1.2	1.21	11.6	.30	542	1805	.24	-
12	2	2.1	.94	65.6	.30	542	1805	.24	-
12	3	1.5	1.05	42.4	.30	542	1805	.24	-
12	4	1.4	1.16	33.5	.30	542	1805	.24	-
13	1	2.8	2.22	13.1	.12	517	4308	.11	-
13	2	2.7	3.11	26.0	.12	517	4308	.11	-
13	3	2.4	2.22	46.3	.12	517	4308	.11	-
13	4	3.1	2.12	33.1	.12	517	4308	.11	-
* 14	1	1.5	1.25	11.6	.28	336	1200	.19	.16
* 14	2	2.7	1.26	66.8	.28	336	1200	.19	.16
* 14	3	1.8	1.23	33.8	.28	336	1200	.19	.16
* 14	4	2.1	1.27	50.9	.28	336	1200	.19	.16
* 15	1	3.4	2.42	11.9	.13	232	1785	.16	.18
* 15	2	3.6	2.40	27.5	.13	232	1785	.16	.18
* 15	3	4.3	2.38	38.7	.13	232	1785	.16	.18
* 15	4	5.7	2.44	52.1	.13	232	1785	.16	.18

* Teflon coat on the bow and waterline side of the hull

Table 24 Continuous-icebreaking resistance tests: 1/36th model test data in synthetic ice—CCGS *Louis S. St. Laurent*

Ice Sheet Number	Run Number	R (kg)	h (cm)	v (cm/sec)	σ_f (kg/cm²)	E (kg/cm²)	E/σ_f	σ_c (kg/cm²)	Friction
1	1	2.7	1.80	5.1	.18	96	533	.41	-
1	2	9.1	1.58	90.0	.18	96	533	.41	-
1	3	5.0	1.40	43.5	.18	96	533	.41	-
2	1	2.7	1.03	12.6	.18	-	-	.20	.56
2	2	10.4	1.03	93.6	.18	-	-	.20	.56
2	3	4.4	1.06	45.0	.18	-	-	.20	.56
3	1	8.8	3.18	7.0	.38	357	940	.42	.53
3	2	21.0	3.19	80.8	.38	357	940	.42	.53
3	3	16.4	3.20	40.1	.38	357	940	.42	.53
4	1	5.4	2.50	5.8	.30	305	1017	.35	-
4	2	19.3	2.50	84.8	.30	305	1017	.35	-
4	3	10.2	2.50	40.8	.30	305	1017	.35	-
5	1	4.9	1.98	7.1	.95	747	786	1.32	-
5	2	13.2	1.98	85.2	.95	747	786	1.32	-
5	3	8.6	1.98	38.6	.95	747	786	1.32	-
6	1	2.4	1.09	6.0	1.21	1489	1230	.92	.44
6	2	9.1	1.08	86.8	1.21	1489	1230	.92	.44
6	3	4.1	1.09	39.6	1.21	1489	1230	.92	.44
7	1	4.2	2.49	5.9	.70	933	1332	.63	.50
7	2	14.8	2.56	77.1	.70	933	1332	.63	.50
7	3	11.0	2.60	38.6	.70	933	1332	.63	.50

Table 25 Results of parametric continuous-icebreaking resistance test—Model "H1" test data

Ice Sheet Number	R (Kg)	h (cm)	v (cm/s)	σ_f (Kg/cm^2)	$\frac{E}{\sigma_f}$	$\frac{v}{\sqrt{gh}}$	$\frac{\sigma_f}{\rho_w gh}$	$\frac{R}{\rho_w gBh^2}$
1	.82	2.03	30	.016	400	.67	7.9	4.65
	1.02	2.03	40	.016	400	.90	7.9	5.78
	1.04	1.98	50	.016	400	1.13	8.1	6.20
	1.27	2.01	60	.016	400	1.35	8.0	7.34
2	1.31	3.42	10	.063	—	.17	18.4	2.62
	1.69	3.42	20	.063	—	.35	18.4	3.33
	1.81	3.39	30	.063	—	.52	18.6	3.68
	2.02	3.29	40	.063	—	.70	19.1	4.36
3	.85	2.17	20	.091	220	.43	41.9	4.22
	.95	2.14	30	.091	220	.66	42.5	4.85
	1.14	2.38	40	.091	220	.83	38.2	4.70
	1.35	2.24	50	.091	220	1.07	40.6	6.29
4	.48	2.54	10	.115	288	.20	45.3	1.74
	.68	2.54	20	.115	288	.40	44.9	2.42
	1.10	2.58	30	.115	288	.60	44.6	3.86
	1.33	2.62	40	.115	288	.96	43.9	4.53
5	.43	.96	40	.094	—	1.30	97.9	10.9
	.54	.93	50	.094	—	1.66	101.	14.6
	.71	.94	60	.094	—	1.98	100.	18.8
	.82	1.01	70	.094	—	2.22	93.	18.8

Table 26 Results of parametric continuous-icebreaking resistance test—Model "B2, H2" test data

Ice Sheet Number	R (Kg)	h (cm)	v (cm/s)	σ_f (Kg/cm^2)	$\frac{E}{\sigma_f}$	$\frac{v}{\sqrt{gh}}$	$\frac{\sigma_f}{\rho_w gh}$	$\frac{R}{\rho_w gBh^2}$
1	.85	1.80	30	.016	400	.71	8.9	6.13
	.99	1.87	40	.016	400	.93	8.6	6.61
	1.13	1.87	50	.016	400	1.17	8.6	7.55
	1.27	1.92	60	.016	400	1.38	8.3	8.05
2	1.35	3.35	10	.063	—	.17	18.8	2.81
	1.79	3.38	20	.063	—	.35	18.6	3.66
	1.89	3.35	30	.063	—	.52	18.8	3.93
	2.47	3.42	40	.063	—	.69	18.4	4.93
3	.99	2.19	20	.079	220	.43	36.1	4.82
	1.10	2.20	30	.079	220	.65	35.9	5.31
	1.18	2.23	40	.079	220	.86	35.4	5.54
	1.41	2.28	50	.079	220	1.06	34.6	6.34
4	.80	2.57	10	.115	288	.20	44.7	2.83
	.97	2.59	20	.115	288	.40	44.4	3.38
	1.25	2.61	30	.115	288	.59	44.1	4.29
	1.51	2.61	40	.115	288	.79	44.1	5.18
5	.48	.91	40	.094	—	1.34	103.	13.5
	.52	.90	50	.094	—	1.68	104.	15.0
	.63	.89	60	.094	—	2.03	106.	18.6
	.76	.92	70	.094	—	2.33	100.	20.9

Table 27 Results of parametric continuous-icebreaking resistance test—Model "H3" test data

Ice Sheet Number	R (Kg)	h (cm)	v (cm/s)	σ_f (Kg/cm^2)	$\frac{E}{\sigma_f}$	$\frac{v}{\sqrt{gh}}$	$\frac{\sigma_f}{\rho_w g h}$	$\frac{R}{\rho_w g B h^2}$
1	1.12	2.07	30	.016	400	.67	7.7	6.11
	1.39	2.05	40	.016	400	.89	7.8	7.73
	1.36	1.99	50	.016	400	1.13	8.1	8.02
	1.60	1.95	60	.016	400	1.37	8.2	10.2
2	1.63	3.33	10	.063	—	.18	18.9	3.43
	1.83	3.31	20	.063	—	.35	19.0	3.90
	2.54	3.34	30	.063	—	.52	18.9	5.32
	3.01	3.57	40	.063	—	.68	17.6	5.52
3	1.31	2.32	20	.091	220	.42	39.2	5.69
	1.44	2.26	30	.091	220	.64	40.3	6.59
	1.67	2.48	40	.091	220	.81	36.7	6.34
	2.16	2.30	50	.091	220	1.05	39.6	9.54
4	.90	2.59	10	.124	288	.20	47.9	3.13
	1.34	2.63	20	.124	288	.39	47.1	4.53
	1.63	2.60	30	.124	288	.59	47.7	5.63
	1.64	2.54	40	.124	288	.80	48.8	5.94
5	.52	.97	40	.094	—	1.30	96.9	12.9
	.71	.99	50	.094	—	1.60	94.9	16.9
	.83	1.02	60	.094	—	1.90	92.2	18.6
	1.01	1.01	70	.094	—	2.22	93.1	23.1

Table 28 Results of parametric continuous-icebreaking resistance test—Model "C1" test data

Ice Sheet Number	R (Kg)	h (cm)	v (cm/s)	σ_f (Kg/cm^2)	$\frac{E}{\sigma_f}$	$\frac{v}{\sqrt{gh}}$	$\frac{\sigma_f}{\rho_w g h}$	$\frac{R}{\rho_w g B h^2}$
1	.74	1.70	30	.016	400	.74	9.41	4.80
	1.02	1.84	40	.016	400	.94	8.70	5.64
	1.09	1.84	50	.016	400	1.18	8.70	6.03
	1.15	1.87	60	.016	400	1.40	8.56	6.16
2.	1.25	3.40	10	.063	—	.17	18.5	2.02
	1.72	3.41	20	.063	—	.35	18.5	2.77
	2.05	3.36	30	.063	—	.52	18.7	3.40
	2.37	3.32	40	.063	—	.70	19.0	4.03
3.	.89	2.13	20	.079	220	.44	37.1	3.67
	.94	2.16	30	.079	220	.65	36.6	3.77
	.99	2.23	40	.079	220	.86	35.4	3.73
	1.14	2.27	50	.079	220	1.06	34.8	4.14
4.	.66	2.67	10	.124	288	.20	46.4	1.73
	.99	2.67	20	.124	288	.39	46.4	2.60
	1.16	2.64	30	.124	288	.59	47.0	3.12
	1.45	2.62	40	.124	288	.79	47.3	3.90
5	.45	1.02	40	.094	—	1.26	92.2	8.10
	.63	1.01	50	.094	—	1.59	93.1	11.6
	.69	1.02	60	.094	—	1.90	92.2	12.4
	.87	1.02	70	.094	—	2.21	92.2	15.7

Table 29 Results of parametric continuous-icebreaking resistance test—Model "C2, B3, L1" test data

Ice Sheet Number	R (Kg)	h (cm)	v (cm/s)	σ_f (Kg/cm^2)	$\frac{E}{\sigma_f}$	$\frac{v}{\sqrt{gh}}$	$\frac{\sigma_f}{\rho_w gh}$	$\frac{R}{\rho_w gBh^2}$
6	1.29	2.31	20	.060	243	.42	26.0	4.53
	1.38	2.28	30	.060	243	.63	26.3	4.97
	1.52	2.30	40	.060	243	.84	26.1	5.39
	1.93	2.31	50	.060	243	1.05	26.0	6.77
7	2.25	3.32	10	.058	241	.18	17.5	3.82
	2.40	3.30	20	.058	241	.35	17.6	4.13
	2.98	3.32	30	.058	241	.53	17.5	5.06
	3.39	3.41	40	.058	241	.69	17.0	5.46
8	1.25	2.00	30	.084	268	.68	42.0	5.85
	1.46	2.07	40	.084	268	.89	40.6	6.38
	1.50	2.09	50	.084	268	1.10	40.2	6.43
	1.87	2.14	60	.084	268	1.31	39.3	7.65
9	2.13	3.12	10	.071	377	.18	22.8	4.10
	2.01	3.01	20	.071	377	.37	23.6	4.15
	1.95	2.84	30	.071	377	.57	25.0	4.53
	2.44	2.97	40	.071	377	.74	23.9	5.18
10	.68	1.01	40	.047	—	1.27	46.5	12.5
	.82	1.05	50	.047	—	1.56	44.8	13.9
	.98	1.03	60	.047	—	1.89	45.6	17.3
	1.08	1.04	70	.047	—	2.19	45.2	18.7

Table 30 Results of parametric continuous-icebreaking resistance test—Model "C3" test data

Ice Sheet Number	R (Kg)	h (cm)	v (cm/s)	σ_f (Kg/cm^2)	$\frac{E}{\sigma_f}$	$\frac{v}{\sqrt{gh}}$	$\frac{\sigma_f}{\rho_w gh}$	$\frac{R}{\rho_w gBh^2}$
6	1.75	2.49	20	.070	243	.41	28.1	5.29
	2.05	2.67	30	.070	243	.59	26.2	5.39
	2.18	2.57	40	.070	243	.80	27.2	6.18
	2.21	2.45	50	.070	243	1.02	28.0	6.89
7	2.16	3.33	10	.058	241	.18	17.4	3.65
	2.27	3.27	20	.058	241	.35	17.7	3.98
	2.71	3.41	30	.058	241	.52	17.0	4.36
	3.47	3.64	40	.058	241	.67	15.9	4.90
8	1.60	2.15	30	.076	268	.65	35.3	6.48
	1.79	2.15	40	.076	268	.87	35.3	7.25
	1.79	2.17	50	.076	268	1.08	35.0	7.12
	2.01	2.16	60	.076	268	1.30	35.2	8.07
9	1.87	2.99	10	.065	377	.19	21.7	3.92
	2.07	2.95	20	.065	377	.37	22.0	4.45
	2.44	2.93	30	.065	377	.56	22.2	5.32
	2.81	2.94	40	.065	377	.75	22.1	6.09
10	.54	.73	40	.064	—	1.49	87.7	19.0
	.79	.83	50	.064	—	1.75	77.1	21.5
	1.15	.97	60	.064	—	1.95	66.0	22.9
	1.10	.95	70	.064	—	2.29	67.4	22.8

Table 31 Results of parametric continuous-icebreaking resistance test—Model "B1" test data

Ice Sheet Number	R (Kg)	h (cm)	v (cm/s)	σ_f (Kg/cm²)	$\frac{E}{\sigma_f}$	$\frac{v}{\sqrt{gh}}$	$\frac{\sigma_f}{\rho_w g h}$	$\frac{R}{\rho_w g B h^2}$
6	1.11	2.49	20	.070	243	.41	28.1	4.79
	1.40	2.65	30	.070	243	.59	26.4	5.33
	1.41	2.63	40	.070	243	.79	26.6	5.45
	1.42	2.33	50	.070	243	1.05	30.0	6.99
7	2.60	3.73	20	.094	241	.33	25.2	5.00
	2.64	3.72	30	.045	241	.50	12.1	5.10
	2.75	3.56	40	.045	241	.68	12.6	5.80
	2.77	3.85	20	.094	241	.33	25.4	5.00
8	1.05	2.11	30	.076	268	.66	36.0	6.31
	1.10	2.12	40	.076	268	.88	35.8	6.54
	1.15	2.10	50	.076	268	1.10	36.2	6.97
	1.37	2.13	60	.076	268	1.31	35.7	8.07
9	1.06	2.97	10	.065	377	.19	21.9	3.21
	1.44	2.93	20	.065	377	.37	22.2	4.48
	1.35	2.90	30	.065	377	.56	22.4	4.29
	1.93	3.01	40	.065	377	.74	21.6	5.70
10	.45	1.04	40	.047	—	1.25	45.2	11.1
	.62	1.09	50	.047	—	1.53	43.1	14.0
	.66	1.07	60	.047	—	1.85	43.9	15.4
	.76	1.12	70	.047	—	2.11	42.0	16.2

Table 32 Results of parametric continuous-icebreaking resistance test—Model "L2" test data

Ice Sheet Number	R (Kg)	h (cm)	v (cm/s)	σ_f (Kg/cm²)	$\frac{E}{\sigma_f}$	$\frac{v}{\sqrt{gh}}$	$\frac{\sigma_f}{\rho_w g h}$	$\frac{R}{\rho_w g B h^2}$
6	1.20	2.18	20	.060	243	.43	27.5	4.73
	1.31	2.16	30	.060	243	.65	27.8	5.20
	1.59	2.14	40	.060	253	.87	28.0	6.50
	1.67	2.11	50	.060	243	1.10	28.4	7.02
7	2.89	3.79	20	.094	241	.33	24.8	3.77
	3.23	3.65	30	.045	241	.50	12.3	4.54
	3.48	3.58	40	.045	241	.68	12.6	5.08
	3.59	3.84	20	.094	241	.33	24.5	4.56
8	1.18	2.07	30	.084	268	.67	40.6	5.16
	1.50	2.14	40	.084	268	.87	39.3	6.13
	1.65	2.15	50	.084	268	1.09	39.1	6.68
	1.87	2.27	60	.084	268	1.27	37.0	6.80
9	1.98	3.13	10	.071	377	.18	22.7	3.78
	2.24	3.08	20	.071	377	.36	23.1	4.42
	1.98	2.92	30	.071	377	.56	24.3	4.35
	2.43	2.99	40	.071	377	.74	23.7	5.09
10	.53	.85	40	.064	—	1.39	75.3	13.7
	.72	.87	50	.064	—	1.71	73.6	17.8
	1.05	1.01	60	.064	—	1.91	63.4	19.3
	.92	.94	70	.064	—	2.31	68.1	19.5

Table 33 Results of parametric continuous-icebreaking resistance test—Model "C2, B3, L1" test data

Ice Sheet Number	R (Kg)	h (cm)	v (cm/s)	σ_f (Kg/cm²)	$\frac{E}{\sigma_f}$	$\frac{v}{\sqrt{gh}}$	$\frac{\sigma_f}{\rho_w gh}$	$\frac{R}{\rho_w gBh^2}$
11	1.59	2.31	20	.059	—	.42	25.5	5.58
	1.95	2.39	40	.059	—	.826	24.7	6.39
12	.49	.81	40	.032	—	1.42	39.5	14.0
	.61	.80	50	.032	—	1.78	40.0	17.8
	.66	.80	60	.032	—	2.14	40.0	19.3
	.70	.78	70	.032	—	2.53	41.0	21.5
13	1.31	2.62	10	.082	682	.20	31.3	3.57
	2.14	2.89	20	.082	682	.38	28.4	4.80
	2.25	2.94	30	.082	682	.56	27.9	4.87
	2.58	2.99	40	.082	682	.74	27.4	5.40
14	1.09	1.88	30	.055	—	.70	29.3	5.78
	1.16	1.94	40	.055	—	.92	28.4	5.77
	1.37	1.85	50	.055	—	1.17	29.7	7.50
	1.42	1.87	60	.055	—	1.40	29.4	7.60
15	.91	2.22	10	.058	657	.21	26.1	3.46
	1.48	2.28	30	.058	657	.63	25.4	5.33
	2.16	2.45	60	.058	657	1.22	23.7	6.74
	2.31	2.46	70	.058	657	1.42	23.6	7.15

Table 34 Results of parametric continuous-icebreaking resistance test—Model "C2, B3, H2, L3" test data

Ice Sheet Number	R (Kg)	h (cm)	v (cm/s)	σ_f (Kg/cm²)	$\frac{E}{\sigma_f}$	$\frac{v}{\sqrt{gh}}$	$\frac{\sigma_f}{\rho_w gh}$	$\frac{R}{\rho_w gBh^2}$
11	1.45	2.38	20	.059	—	.41	24.8	4.79
	2.01	2.40	40	.059	—	.82	24.6	6.53
12	.54	.89	40	.032	—	1.35	36.0	12.8
	.68	.89	50	.032	—	1.69	36.0	16.1
	.85	.87	60	.032	—	2.05	36.8	21.0
	.83	.89	70	.032	—	2.37	36.0	19.6
13	1.55	2.65	10	.082	682	.20	30.9	4.13
	2.27	2.94	20	.082	682	.37	27.9	4.92
	2.75	3.03	30	.082	682	.55	27.1	5.61
	2.91	3.02	40	.082	682	.74	27.2	5.97
14	1.25	1.90	30	.055	—	.70	28.9	6.48
	1.44	1.89	40	.055	—	.93	29.1	7.55
	1.78	1.91	50	.055	—	1.16	28.8	9.14
	1.76	1.92	60	.055	—	1.38	28.6	8.94
15	1.77	2.31	10	.058	657	.21	25.1	2.72
	1.42	2.38	30	.058	657	.62	24.4	4.69
	2.20	2.45	60	.058	657	1.22	23.7	6.86
	2.75	2.49	70	.058	657	1.42	23.3	8.31

Table 35 Results of parametric continuous-icebreaking resistance test—Model "C2, B3, H2, L3" test data

Ice Sheet Number	R (Kg)	h (cm)	v (cm/s)	σ_f (Kg/cm²)	$\frac{E}{\sigma_f}$	$\frac{v}{\sqrt{gh}}$	$\frac{\sigma_f}{\rho_w g h}$	$\frac{R}{\rho_w g B h^2}$
11	1.45	2.39	20	.074	—	.413	31.0	4.75
	1.80	2.34	40	.074	—	.84	31.6	6.16
	2.28	2.54	50	.074	—	1.00	29.1	6.65
12	.55	.82	40	.032	—	4.41	39.0	15.3
	.74	.85	60	.032	—	2.08	37.6	19.2
	.79	.86	70	.032	—	2.41	37.2	20.0

Table 36 Icebreaking maneuvering test results—*Wind* model test data

ICE THICK cm	TOW SPEED cm/sec	DRIFT ANGLE degrees	ARM LENGTH cm	FORCE X kg	FORCE Y kg	MOMENT N kg/cm	u cm/sec	v cm/sec	r rad/sec	σ_f kg/cm²
LABRADOR 1 STRAIGHT LINE TEST 8-22-75										
1.20	108.54	0.	0.	-2.56	-0.23	0.0	108.54	0.00	0.000	0.15
1.33	108.54	-1.	0.	-2.56	-1.84	-73.0	108.52	1.89	0.000	0.15
1.35	108.54	1.	0.	-2.68	0.27	13.0	108.52	-1.89	0.000	0.15
1.37	108.54	4.	0.	-2.64	1.56	76.6	108.34	-6.63	0.000	0.15
1.40	106.13	6.	0.	-2.79	2.05	104.8	105.64	-10.17	0.000	0.15
1.33	108.54	2.	0.	-2.56	0.82	34.4	108.47	-3.79	0.000	0.15
1.28	106.13	8.	0.	-2.54	2.76	134.5	105.10	-14.77	0.000	0.15
LABRADOR 1 ROTATING ARM TEST 8-20-75										
0.99	-106.90	0.	292.	-1.50	2.31	328.0	-106.90	0.00	-0.366	0.10
0.94	-98.70	0.	371.	-1.84	1.50	205.6	-98.70	0.00	-0.266	0.10
1.07	-95.70	0.	458.	-2.06	1.34	181.4	-95.70	0.00	-0.209	0.10
0.96	-54.00	0.	458.	-1.03	0.50	51.7	-54.00	0.00	-0.118	0.10
LABRADOR 2 STRAIGHT LINE TEST 8-22-75										
1.07	86.80	0.	0.	-1.72	-0.10	0.0	86.80	0.00	0.000	0.14
1.07	86.80	-1.	0.	-1.60	-0.41	-5.2	86.79	1.51	0.000	0.14
1.08	86.80	1.	0.	-1.54	0.45	7.8	86.79	-1.51	0.000	0.14
1.13	86.80	4.	0.	-1.60	1.10	30.8	86.64	-5.30	0.000	0.14
1.08	86.80	6.	0.	-1.68	1.43	50.0	86.40	-8.32	0.000	0.14
1.06	86.80	2.	0.	-1.56	0.51	17.2	86.75	-3.03	0.000	0.14
0.96	86.80	8.	0.	-1.29	1.76	81.8	85.96	-12.08	0.000	0.14
LABRADOR 2 ROTATING ARM TEST 8-21-75										
1.03	27.70	0.	458.	-0.86	-0.56	-20.3	27.70	0.00	0.061	0.29
1.03	70.10	0.	458.	-1.52	-1.19	-96.9	70.10	0.00	0.153	0.19
1.08	77.70	0.	371.	-1.89	-1.24	-151.7	77.70	0.00	0.209	0.06
1.05	85.60	0.	292.	-2.02	-1.93	-241.8	85.60	0.00	0.293	0.12

(Cont'd)

ICE THICK cm	TO SPE cm									
MODEL 1										
1.22	37									
1.20	37									
1.21	36									
1.19	37									
1.25	36.									
1.43	37.									
MODEL 1 RE										
1.42	38.									
1.79	35.									
1.71	32.									
MODEL 2 ST										
1.14	37.									.06
1.37	37.									.06
1.57	37.									.06
1.57	37.									.06
1.49	37.									.06
1.50	37.									.06
MODEL 2 RE										
1.32	-32.									.16
1.41	-34.									.06
1.07	-37.									.05
MODEL 3 ST										
1.26	15.									.09
1.45	15.									.09
1.73	14.									.09
1.79	14.									.09
1.68	15.									.09
1.70	15.									.00
MODEL 3 RE										
1.34	-31.									.10
1.43	-36.									.10
1.44	-40.									.10

MODEL 1 STRAIGHT LINE TEST IN THICK ICE 8-1-75

2.20	14.92	0.	0.	-1.23	0.42	0.0	14.92	0.00	0.000	0.09
2.69	14.92	3.	0.	-1.76	1.78	7.3	14.90	-0.78	0.000	0.09
2.93	13.65	9.	0.	-2.19	5.58	47.5	13.48	-2.14	0.000	0.09
2.96	16.08	2.	0.	-1.97	0.95	6.4	16.07	-0.42	0.000	0.09
2.72	15.92	6.	0.	-2.01	3.99	30.5	15.83	-1.66	0.000	0.09
2.64	15.01	-3.	0.	-1.83	1.78	-9.8	14.99	0.79	0.000	0.09

MODEL 1 ROTATING ARM TEST IN THICK ICE 8-4-75

2.46	19.20	0.	458.	-2.61	-1.45	-92.8	19.20	0.00	0.042	0.09
2.84	17.40	0.	371.	-2.83	-0.58	-206.9	17.40	0.00	0.047	0.14
3.15	16.90	0.	292.	-2.84	-1.78	-178.2	16.90	0.00	0.058	0.09

Table 36 (*Continued*)

WIND MODEL AND PARAMETRIC MODEL (CONT.) NONDIMENSIONAL DATA

$\frac{X}{\rho_w g B h^2}$	$\frac{Y}{\rho_w g B h^2}$	$\frac{N}{\rho_w g B L h^2}$	$\frac{U}{\sqrt{gh}}$	$\frac{V}{\sqrt{gh}}$	$\frac{r}{\sqrt{g/h}}$	$\frac{\sigma_t}{\rho_w g h}$
MODEL 1 STRAIGHT LINE TEST IN THICK ICE						
-4.764	1.631	0.000	0.321	0.000	0.0000	38.6
-4.560	4.612	0.079	0.290	-0.015	0.0000	31.6
-4.783	12.186	0.434	0.252	-0.040	0.0000	29.0
-4.215	2.033	0.057	0.298	-0.008	0.0000	28.7
-5.093	10.111	0.323	0.307	-0.032	0.0000	31.2
-4.923	4.788	-0.110	0.295	0.015	0.0000	32.2
MODEL 1 ROTATING ARM TEST IN THICK ICE						
-8.086	-4.492	-1.202	0.392	0.000	0.0021	36.6
-6.578	-1.348	-2.010	0.330	0.000	0.0025	49.3
-5.366	-3.363	-1.407	0.305	0.000	0.0033	28.6
LABRADOR 1 STRAIGHT LINE TEST						
-33.908	-3.046	0.000	3.164	0.000	0.0000	125.0
-27.603	-19.840	-3.720	3.005	0.052	0.0000	0.0
-28.047	2.857	0.645	2.983	-0.052	0.0000	111.1
-26.828	15.853	3.681	2.956	-0.181	0.0000	73.0
-27.150	19.949	4.819	2.851	-0.275	0.0000	0.0
-27.603	8.874	1.753	3.004	-0.105	0.0000	75.2
-29.569	32.130	7.400	2.966	-0.417	0.0000	0.0
LABRADOR 1 ROTATING ARM TEST						
-29.190	44.953	30.175	-3.430	0.000	-0.0116	101.0
-39.718	32.378	20.980	-3.250	0.000	-0.0082	106.4
-34.318	22.323	14.286	-2.955	0.000	-0.0069	93.5
-21.316	10.348	5.058	-1.761	0.000	-0.0037	104.2
LABRADOR 2 STRAIGHT LINE TEST						
-28.654	-1.649	0.000	2.680	0.000	0.0000	130.8
-26.655	-6.897	-0.410	2.679	0.047	0.0000	130.8
-25.182	7.375	0.605	2.667	-0.047	0.0000	129.6
-23.899	16.431	2.171	2.603	-0.159	0.0000	123.9
-27.471	23.383	3.868	2.655	-0.256	0.0000	129.6
-26.481	8.623	1.380	2.691	-0.094	0.0000	132.1
-26.697	36.424	8.006	2.802	-0.394	0.0000	145.8
LABRADOR 2 ROTATING ARM TEST						
-15.461	-10.068	-1.725	0.872	0.000	0.0020	281.6
-27.327	-21.394	-8.236	2.206	0.000	0.0050	184.5
-30.905	-20.277	-11.727	2.387	0.000	0.0069	55.6
-34.946	-38.389	-19.775	2.668	0.000	0.0096	114.3

PARAMETRIC MODEL NONDIMENSIONAL DATA

$\frac{X}{\rho_w g B h^2}$	$\frac{Y}{\rho_w g B h^2}$	$\frac{N}{\rho_w g B L h^2}$	$\frac{u}{\sqrt{gh}}$	$\frac{v}{\sqrt{gh}}$	$\frac{r}{\sqrt{g/h}}$	$\frac{\sigma_t}{\rho_w g h}$
MODEL 1 STRAIGHT LINE TEST IN THIN ICE						
-9.951	0.504	0.172	1.090	0.000	0.0000	106.6
-10.415	10.936	0.651	1.095	-0.057	0.0000	108.3
-10.244	18.823	0.873	1.058	-0.168	0.0000	107.4
-9.797	16.019	0.843	1.083	-0.114	0.0000	109.2
-8.759	22.317	0.982	1.028	-0.219	0.0000	104.0
-8.068	-9.901	-0.508	0.992	0.052	0.0000	69.9
MODEL 1 ROTATING ARM TEST IN THIN ICE						
-9.855	-10.041	-2.514	1.020	0.000	0.0032	89.4
-4.388	-6.846	-1.837	0.846	0.000	0.0041	49.7
-8.399	-6.668	-2.069	0.792	0.000	0.0046	32.2
MODEL 2 STRAIGHT LINE TEST						
-12.695	1.284	0.000	1.128	0.000	0.0000	52.6
-9.289	10.987	0.559	1.027	-0.054	0.0000	43.8
-10.040	18.102	0.788	0.944	-0.150	0.0000	38.2
-9.355	17.722	0.744	0.945	-0.099	0.0000	38.2
-9.627	22.800	0.942	0.954	-0.203	0.0000	40.3
-8.416	-10.082	-0.414	0.971	0.051	0.0000	40.0
MODEL 2 ROTATING ARM TEST						
-9.576	3.981	3.642	-0.892	0.000	-0.0040	121.2
-6.035	1.509	2.187	-0.940	0.000	-0.0036	42.6
-9.497	2.784	2.012	-1.144	0.000	-0.0026	46.7
MODEL 3 STRAIGHT LINE TEST						
-5.078	0.472	0.000	0.440	0.000	0.0000	69.0
-5.974	8.649	0.068	0.399	-0.021	0.0000	60.0
-6.890	15.535	0.057	0.358	-0.057	0.0000	50.3
-5.793	11.995	0.000	0.354	-0.037	0.0000	48.6
-5.447	16.008	0.049	0.366	-0.078	0.0000	51.8
-4.346	-5.709	-0.123	0.372	0.019	0.0000	0.0
MODEL 3 ROTATING ARM TEST						
-8.248	16.705	4.433	-0.878	0.000	-0.0040	74.6
-7.609	14.027	3.717	-0.967	0.000	-0.0037	69.9
-6.238	12.658	3.543	-1.070	0.000	-0.0033	69.4